

# Light-Powered Microrobots: Challenges and Opportunities for Hard and Soft Responsive Microswimmers

Ada-Ioana Bunea,\* Daniele Martella, Sara Nocentini, Camilla Parmeggiani, Rafael Taboryski, and Diederik S. Wiersma

Worldwide research in microrobotics has exploded in the past two decades, leading to the development of microrobots propelled in various manners. Despite significant advances in the field and successful demonstration of a wide range of applications, microrobots have yet to become the preferred choice outside a laboratory environment. After introducing available microrobotic propulsion and control mechanisms, microrobots that are manufactured and powered by light are focused herein. Referring to pioneering works and recent interesting examples, light is presented not only as a fabrication tool, by means of two-photon polymerization direct laser writing, but also as an actuator for microrobots in both hard and soft stimuli-responsive polymers. In this scenario, a number of challenges that yet prevent polymeric light-powered microrobots from reaching their full potential are identified, whereas potential solutions to overcome said challenges are suggested. As an outlook, a number of real-world applications that light-powered microrobots should be particularly suited for are mentioned, together with the advances needed for them to achieve such purposes. An interdisciplinary approach combining materials science, microfabrication, photonics, and data science should be conducive to the next generation of microrobots and will ultimately foster the translation of microrobotic applications into the real world.

objects that perform specific microscale tasks autonomously or under external control. This type of devices are often referred to in literature as microrobots, but they have also been called micro- or nanomachines, motors, rotors, swimmers, or tools. Regardless of the term used in the original works covered herein, this Review instead systematically uses the term *microrobot*, both to improve the text flow and to emphasize the task-oriented aspect.

Due to technological advancements, the beginning of the 21st century marked the start of a new era for microtechnology, and a plethora of microrobots of different shapes and sizes have been developed ever since, using a variety of materials, fabrication technologies, and control methods. Thus, research in microrobotics is a relatively recent field that has been growing at an accelerated rate in the past few years. **Figure 1** shows the number of publications containing the terms *microrobot*, *nanorobot*, and *microswimmer* from the beginning of 2000 according to a ScienceDirect search conducted in mid-December 2020.

Unfortunately, other relevant terms, i.e., *microtool* and *micro-/nanomachine*, cannot be included in the graph due to an overlap in the use of such terms with research not related to the type of microrobots discussed herein. Please note that the term *microswimmer* emerged in the past decade and is used for microorganisms such as bacteria, as well as microrobots that

## 1. Introduction

A robot is defined in the Oxford English Dictionary as a *machine capable of carrying out a complex series of actions automatically, especially one programmable by a computer*. In the context of this Review, the term *microrobot* is used for submillimeter untethered


Dr. A.-I. Bunea, Prof. R. Taboryski  
National Centre for Nano Fabrication and Characterization  
(DTU Nanolab)  
Technical University of Denmark  
Ørsted Plads 347, Lyngby 2800 Kgs., Denmark  
E-mail: adabu@dtu.dk

Dr. A.-I. Bunea, Dr. D. Martella, Dr. S. Nocentini, Dr. C. Parmeggiani,  
Prof. D. S. Wiersma  
European Laboratory for Non-Linear Spectroscopy (LENS)  
University of Florence  
via Nello Carrara 1, Sesto Fiorentino 50019, Italy

Dr. D. Martella, Dr. S. Nocentini, Prof. D. S. Wiersma  
Istituto Nazionale di Ricerca Metrologica (INRiM)  
Strada delle Cacce 91, Torino 10135, Italy

Dr. C. Parmeggiani  
Chemistry Department "Ugo Schiff"  
University of Florence  
via della Lastruccia 3-13, Sesto Fiorentino 50019, Italy

Prof. D. S. Wiersma  
Physics and Astronomy Department  
University of Florence  
via Nello Carrara 1, Sesto Fiorentino 50019, Italy

 The ORCID identification number(s) for the author(s) of this article can be found under <https://doi.org/10.1002/aisy.202000256>.

© 2021 The Authors. Advanced Intelligent Systems published by Wiley-VCH GmbH. This is an open access article under the terms of the Creative Commons Attribution License, which permits use, distribution and reproduction in any medium, provided the original work is properly cited.

DOI: 10.1002/aisy.202000256

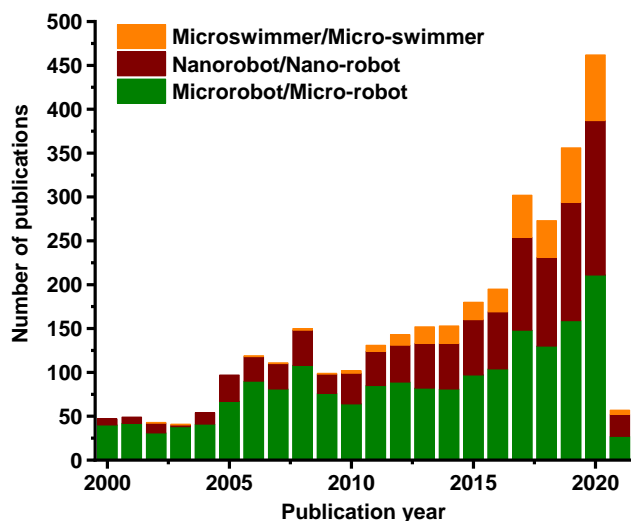


**Figure 1.** Number of publications containing the terms microswimmer or micro-swimmer, nanorobot or nano-robot, and microrobot or micro-robot, from January 2000 to the December 11, 2020, according to ScienceDirect. There is a clear trend showing an increasing interest in such microscopic objects in recent years.

move in liquid environments. Nevertheless, the retrieved data show a clear trend for an increasing interest in micro- and nanorobotics in recent years.

Early examples of microrobots taking advantage of polymeric materials include a polypyrrole/gold-based microrobotic arm controlled by electrical currents,<sup>[1]</sup> and 3D-printed polymer objects trapped and rotated using focused laser beams.<sup>[2]</sup> In the same period, inorganic compounds were explored to fabricate optically controllable SiO<sub>2</sub> micromachined elements,<sup>[3]</sup> autonomous metallic Janus nanorods made of gold and platinum,<sup>[4]</sup> or gold and nickel.<sup>[5]</sup> Only a few years later, biological materials were used as microrobot constituents, for building biohybrid microrobots consisting of red blood cells attached to flexible magnetic filaments using biotid/streptavidin interactions.<sup>[6]</sup>

In 2005, Ozin et al. asked an interesting question about microrobots: *Are these just nanomachine dreams, or dream nanomachines?*<sup>[7]</sup> Since 2005, significant progress has been made in the field and many applications have indeed been demonstrated. For example, in 2013, Mg-based water-fueled Janus microrobots<sup>[8]</sup> and Fe/Pt microrobots fueled by hydrogen peroxide<sup>[9]</sup> were reported for the removal of water pollutants, whereas Mg-based Janus microrobots with biocompatible propulsion were suggested to have interesting biomedical applications.<sup>[10]</sup> The same year, magnetic microrobots for cellular manipulation were described.<sup>[11]</sup> In 2015, autonomous microrobots were used for sensing,<sup>[12]</sup> cargo transport through blood,<sup>[13]</sup> and rewiring of cracked microelectrodes.<sup>[14]</sup> More recent microrobot studies focus mostly on biomedical<sup>[15–20]</sup> and environmental<sup>[21]</sup> applications. A number of recent review articles cover various types of microrobots and their applications. Interested readers are referred to those discussing microrobots for biomedical applications,<sup>[22–28]</sup> the use of microrobots in analytical chemistry,<sup>[29]</sup> the fabrication and applications of self-propelled

microrobots,<sup>[30]</sup> the relation between microrobots and electrochemistry,<sup>[31]</sup> microrobots in bioengineering applications,<sup>[32]</sup> catalytic microrobots for biomedical and environmental applications,<sup>[33]</sup> and applications in sensing and removal.<sup>[34]</sup>

Although such a variety of applications has already been demonstrated, unravelling the potential of microrobots has only just begun. Currently, microrobots are rarely the best solution to a given challenge, and there are yet many technical difficulties in both their fabrication and control. For example, from a fabrication perspective, complex multimaterial structures are rather difficult to achieve,<sup>[35]</sup> whereas in terms of control, adaptive locomotion based on effective locomotory gaits is still quite challenging.<sup>[36]</sup> As these challenges are finally overcome and the young field of microrobots matures, we expect a truly disruptive impact in many areas of the technical and natural sciences.

This Review bridges the gap between the parallel development tracks for various microrobots amenable to actuation using light, and particularly for those made of polymeric materials. We believe that, in addition to exploiting knowledge from both the hard and soft light-controlled microrobot development tracks, rapid progress in the field could be achieved by synergistically exploiting knowledge from different scientific research fields, including microfabrication, materials science, chemistry, photonics, and data science. This promising congruency between researchers working on different types of microrobots should lead to a comprehensive vision on functional microrobotics, where transversal limitations could be overcome by innovative solutions.

This Review describes the state of the art, challenges, and envisioned applications of microrobots in fluids, with focus on light-powered microrobots. The study starts by giving an overview of reported microrobotic applications in liquid environments before moving on to propulsion means and control modalities, including the use of light as actuator. Light-powered microrobots are then described in terms of fabrication, optical manipulation, and applications, with focus on polymeric materials for both hard and soft microrobots. Known challenges and potential solutions for improved microrobot locomotion are then discussed, highlighting important issues to consider when designing light-powered microrobots able to accomplish new tasks. The envisioned applications of light-powered microrobots are presented at the end of the review.

### 1.1. Microrobots in Motion

Both autonomous and user-controlled microrobots need a source of energy to be able to move at the microscale. Some microrobots use the fuel available in their environment, whereas others are powered by one or more external sources. The most common microrobot propulsion and control modalities are shown in **Figure 2** and briefly discussed in the following paragraphs, whereas a more detailed comparison between them can be found in other review articles.<sup>[24,37]</sup>

As nature is a big source of inspiration in modern scientific research, microrobots are often designed to mimic the shapes of biological entities or to use similar propulsion mechanisms. Furthermore, a number of biohybrid microrobots that include a living biological swimmer component have been developed.

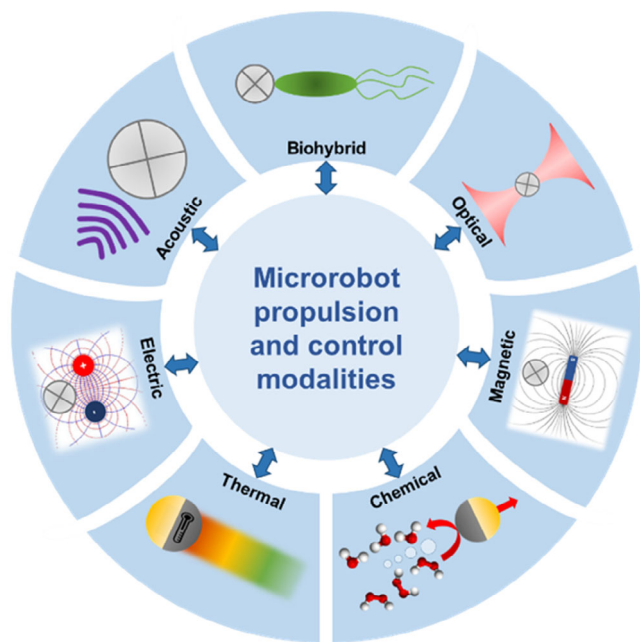


**Figure 2.** The most common microrobot propulsion and control modalities: biohybrid, optical, magnetic, chemical, thermal, electric, or acoustic. Well-known forces and processes are tailored to achieve the desired microscale manipulation.

Among these, bacteria-based microrobots are the most common, whereas other living entities such as algae, sperm cells, contractile, and immune cells have been used.<sup>[38,39]</sup> Biohybrid microrobots are propelled by the living component, which may rely on different swimming mechanisms and use various physicochemical cues for orientation, as recently explained by Alapan et al.<sup>[39]</sup> Although biohybrid propulsion works well for microrobots in laboratory conditions, achieving motion in biological samples or compatibility with the human body is still quite challenging.

The theory behind the use of magnetic fields for microstructure manipulation is explained in details in Rikken et al.<sup>[40]</sup> For magnetic control, the microrobot body can be made of either hard or relatively soft materials, as long as these have suitable magnetic properties.<sup>[41]</sup> Most magnetic microrobots reported to date are either helical, include flexible components, or can act as surface walkers, but other examples have also been reported.<sup>[42]</sup> A biohybrid red blood cell–magnetic flagella system was reported as early as 2005.<sup>[6]</sup> Other hybrid magnetic microrobots include magneto-optical microrobots,<sup>[43]</sup> magnetoacoustic microrobots,<sup>[44]</sup> pH-responsive magnetic microrobots,<sup>[45]</sup> and thermoelectromagnetic microrobots.<sup>[46]</sup> Among the different microrobotic control modalities, magnetic actuation is arguably the most suited for *in vivo* applications due to the ability of magnetic fields to penetrate deeply within tissues, with minimal invasiveness or health risks. Combining the advantages of magnetic actuation with those of other types of control, such as optical control, might hold the key for advancing the field, as recently emphasized by Sitti and Wiersma.<sup>[41]</sup>

The different mechanisms that can be involved in chemically induced microrobot motion have been extensively described in

previous studies.<sup>[47,48]</sup> The first demonstrations of chemically powered microrobots required relatively high concentrations of  $H_2O_2$ ,<sup>[4,5]</sup> which made them unlikely candidates for biological or environmental applications. However, more recent developments include better candidates, such as microrobots powered by enzymatic reactions<sup>[49,50]</sup> water conversion reactions,<sup>[8,51]</sup> and bodily fluids, such as gastric acid or intestinal fluid.<sup>[26,52]</sup>

Thermal, electric,<sup>[25,31,53]</sup> and acoustic<sup>[25,32,54]</sup> control are less explored compared with the aforementioned propulsion and control modalities, and they are often coupled with a different actuating force. Interesting examples of thermoresponsive<sup>[55]</sup> and thermomagnetic<sup>[56]</sup> microrobots have been reported for surgical applications, and a thermoelectromagnetic microrobot was developed for drug delivery.<sup>[46]</sup>

Given the focus of this Review on light-powered microrobots, optical control is described in the following section.

## 2. Light-Based Ingredients

### 2.1. Light as Microrobot Actuator—More than a Power Source

Optical actuation is very versatile, as many different properties of light can be tailored with high spatio-temporal precision. Light offers long range, rapid, precise, and robust control, which can be adjusted in real time. Typically, light is an ideal actuator in simple aqueous solutions, but encounters significant challenges in biological fluids and tissues or other complex media due to absorption and scattering. Despite these challenges, the extremely high precision achievable for manipulation together with the many options for parametrization recommend optical actuation as one of the most valuable microrobotic control modalities. **Figure 3** shows the ultraviolet (UV), visible and infrared (IR) electromagnetic radiation spectrum and highlights the relevant range for powering microrobots.

The oldest and most straightforward approach for microrobotic manipulation is the use of optical trapping. Pioneered by Ashkin in 1970,<sup>[57]</sup> optical trapping is an ever-growing field recently recognized through the 2018 Nobel prize in physics. Optical trapping deals with the precise manipulation of microscale objects of various shapes, materials and origins, including metallic nanoparticles, polymeric microspheres, and living cells. The basic principles of optical trapping and different trapping configurations were recently reviewed by Bunea and Glückstad.<sup>[58]</sup> Briefly, highly focused laser beams generate a strong electric field gradient, which pulls a target object toward the beam focus. If the gradient forces overcome opposing forces, such as scattering forces, Stokes' drag force, and Brownian motion, the object can be stably trapped in the beam focus. Gradually displacing the beam in 3D causes the trapped object to follow the beam focus, which can be exploited for manipulating microrobots with nanometric precision. Typically, optical trapping uses laser light in the near-infrared (nIR) wavelength range, most commonly at wavelengths between 1060 and 1090 nm (Figure 3). The nIR range is preferred as it can ensure stable trapping while minimizing the risk of photodamage for the trapped objects.

Another optical manipulation approach is the use of light to induce changes in the material properties of the microrobot,

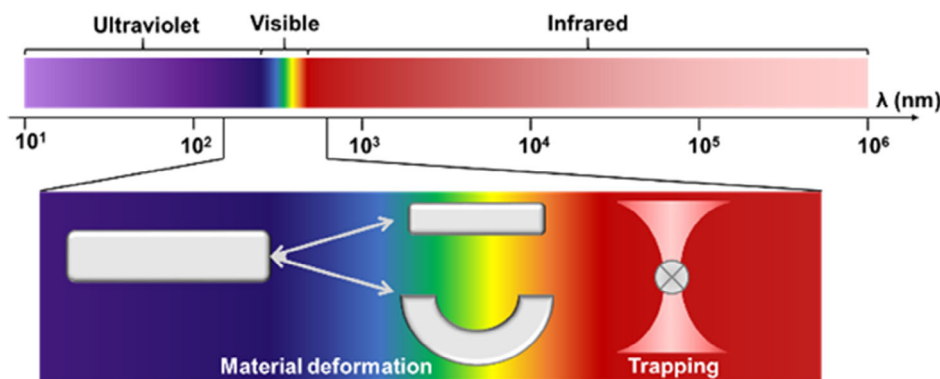


**Figure 3.** Light spectrum by wavelength: from the UV range (10–400 nm) to visible (400–700 nm) and infrared (700–1 mm). The enlarged area shows the spectral range for optical actuation: UV light with a wavelength above 200 nm and/or visible light can be used to induce material deformation in photo-responsive shape-changing materials. The nIR range is typically used for optical trapping, most commonly at wavelengths between 1060 and 1090 nm.

which in turn leads to motion for cleverly engineered objects. This requires microrobotic components made of light-responsive polymers, i.e., shape-changing materials that deform when exposed to light at a certain wavelength. Microrobotic actuation can be based on multicolor illumination, polarization of light, or spatial patterning of light.<sup>[41]</sup> Shape-changing materials are usually responsive to wavelengths in the UV or visible light range (Figure 3).<sup>[59]</sup> Due to the great interest toward the use of nIR in biological applications, shape-changing materials responsive to nIR wavelengths are currently being investigated.<sup>[60,61]</sup> The light intensity typically used to activate the shape changing operation of soft robots is around tens of milliWatts at the laser focus,<sup>[62]</sup> similar to that used for the optical manipulation of hard microrobots.<sup>[63]</sup>

Finally, light can be exploited for inducing microrobot-mediated effects, due to, e.g., photocatalytic,<sup>[21]</sup> or thermoplasmonic<sup>[63]</sup> responses, or it can be used to induce effects leading to phototactic microrobot behaviors, such as propulsion by a self-electrophoresis mechanism.<sup>[64]</sup> In these cases, light does not act as the primary microrobot energy source, but rather as an actuator that drives a further activation mechanism.

Many microrobot examples discussed in this Review are manipulated by means of optical trapping, using either holographic optical tweezers (HOTs),<sup>[65–67]</sup> or the Biophotonics WorkStation (BWS)<sup>[68]</sup> developed at the Technical University of Denmark. The optical setup schematics and trapping principle for HOT and the BWS are shown in Figure 4. HOT setups and the BWS are able to generate multiple simultaneously reconfigurable trapping beams with the aid of a computer-controlled spatial light modulator (SLM). This allows optical manipulation with six degrees of freedom for objects with at least three trapping handles. Typically, HOT use high numerical aperture (NA) objectives and generate relatively high trapping forces. In HOT, each object, i.e., microrobot component, is trapped in the focal point of one of the trapping beams (Figure 4A). The BWS instead uses generalized phase contrast (GPC)-shaped<sup>[69]</sup> counter-propagating beams focused into the sample through lower NA objectives and provides lower trapping forces than HOT, but wider field and depth of view. In the BWS, each object, i.e., microrobot component, is trapped in between the focal points for a pair

of counter-propagating beams (Figure 4B). An alternative to the more expensive HOT for microrobot manipulation is the inclusion of acousto-optic deflectors in a standard optical tweezers setup.<sup>[70]</sup> Whereas this approach enables simultaneous generation of multiple traps, all of the traps are in the same plane, making it impossible to induce microrobot out-of-plane rotation directly. Intelligent microrobot design for distributed force control can overcome this and enable optical manipulation with six degrees of freedom despite the planar optical trap positions.<sup>[71]</sup>

Another noteworthy light-based approach for microstructure manipulation is the use of optoelectronic tweezers.<sup>[72–74]</sup> Recently, polymeric cogwheel-shaped microrobots controlled by optoelectronic tweezers were used for indirect cellular manipulation.<sup>[75]</sup> For the same light intensity, optoelectronic tweezers provide stronger manipulation forces compared with optical tweezers. In addition, the light patterns needed for optoelectronic tweezers can be produced using consumer-grade optical projectors, which makes the technique more accessible than HOTs, while still allowing for parallel manipulation. Overall, despite being explored very little for microrobotics, optoelectronic tweezers might provide improved manipulation solutions.

## 2.2. Light as Microrobot Builder: Two-Photon Polymerization

Two-photon polymerization (2PP) relies on two-photon excitation, a process which was first described theoretically by Göppert-Mayer in 1931<sup>[76]</sup> and experimentally demonstrated 30 years later by Kaiser and Garrett,<sup>[77]</sup> after the invention of the laser. Direct laser writing (DLW) using 2PP was pioneered in the late 1990s<sup>[78]</sup> and is currently the highest-resolution 3D printing technique available, enabling the fabrication of complex structures with features below 200 nm.<sup>[79,80]</sup> In standard photolithography processes, photoresist initiation is triggered by absorption of a high-energy photon (UV wavelength). 2PP instead requires rapid subsequent absorption of two photons of lower energies (nIR wavelength). Whereas for single-photon excitation, there is a linear correlation between the photon density and the reaction speed,<sup>[78]</sup> 2PP is a nonlinear optical process,

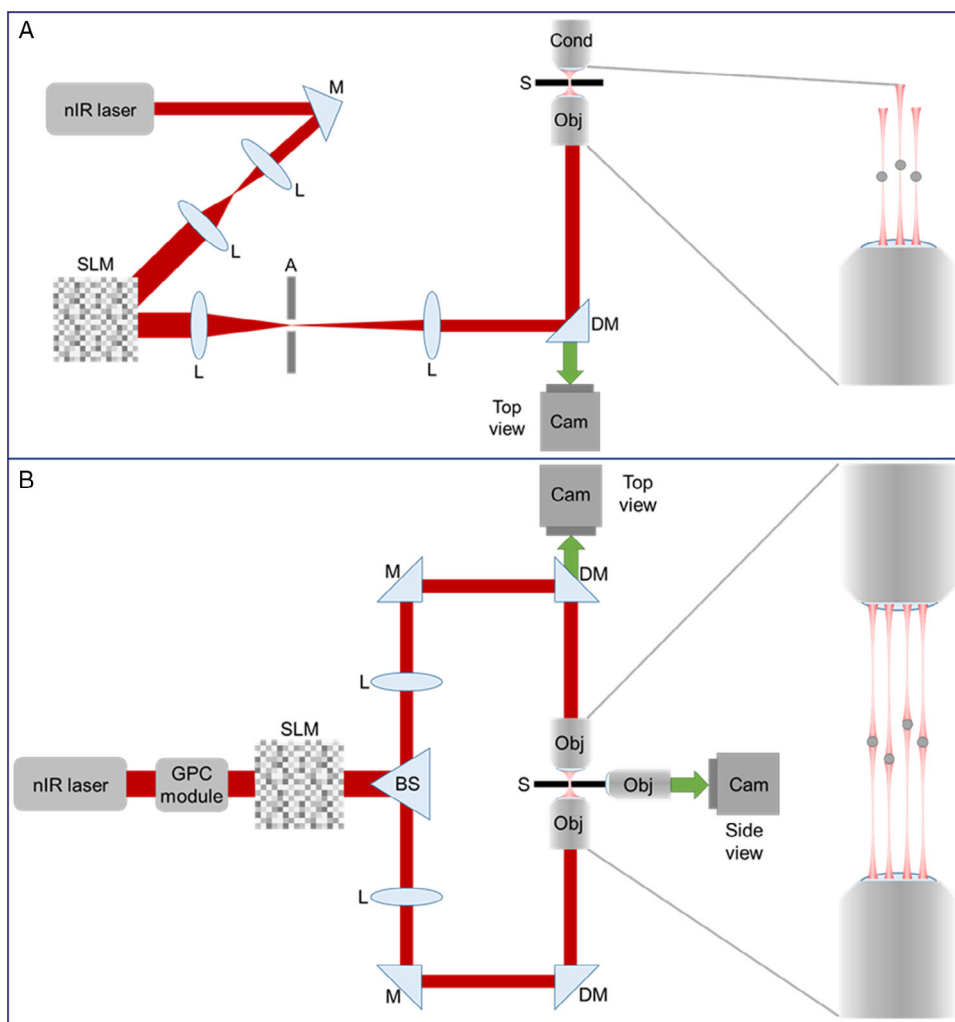


**Figure 4.** Optical setup and trapping principle schematic representation. The nIR light path used for trapping is shown in red, whereas the visible light source and light path are omitted to simplify the schematics. M—mirror; DM—dichroic mirror; L—lens; SLM—spatial light modulator; A—aperture; Cam—camera; Obj—objective; Cond—condenser; S—sample; BS—beamsplitter. A) A generic HOTS setup. The Gaussian beam coming from a nIR laser is expanded using a series of lenses to match the size of the active area of the SLM. The aperture ensures filtering of all diffraction orders in addition to the first diffraction order used for trapping, and a high NA objective enables the beam focusing and optical trapping in the sample. The objects are trapped in the beam focus. Setups from different research groups may include other components or omit the beam expander, but the operating principle remains the same. B) The Biophotonics Workstation (BWS) developed at the Technical University of Denmark. The Gaussian beam coming from a 1080 nm laser is first shaped using a GPC module,<sup>[69]</sup> and then reaches the SLM. The shaped beam is then split into two beams of equal intensity using a 50/50 beamsplitter, and eventually relayed onto the sample from opposite directions using two 50× objectives with a NA of 0.55. This leaves space in the system for a 20× side-view objective. The objects are trapped in between the foci of the top and bottom counter-propagating beams.

for which the polymerization rate is proportional to the square of the photon density in each point of the photoresist. Therefore, polymerization in 2PP occurs almost exclusively in the focused region of high optical density, enabling subdiffraction resolution.

The disruptive power of 2PP has been exploited in different research areas, and 2PP is also a key player in the development of light-powered microrobots. Early commercial 2PP equipment was quite slow, but recent technological advancements have reduced printing time tremendously, which should further promote research activities on 3D-printed microrobots. Today, 2PP is the main technique for the fabrication of light-powered microrobots in both hard and soft polymers, as it enables full

3D design freedom and a printing resolution of <200 nm in the XY plane. However, the resolution is different across the 3D space (XY plane vs Z axis, corresponding to the direction for the propagating laser beam). The focal laser spot has an ellipsoidal shape whose aspect ratio, i.e., ratio between the major and the minor axis dimension, depends on the NA of the laser-focusing objective. Thus, the voxel aspect ratio varies between 1.5 and 3.5, meaning that the resolution is 1.5–3.5 times lower on the Z-axis compared with the XY plane. Voxel optimization was recently described in previous studies.<sup>[81]</sup>

Typically, high-resolution DLW proceeds by 2PP of a negative photoresist in the focal spot of a femtosecond pulsed laser.

Different suitable photoresists based on, e.g., epoxy or acrylate chemistry are commercially available for 2PP, whereas in-house mixtures are also common. While 2PP DLW allows the fabrication of complex structures in different materials, additional microrobot functionalities can be facilitated by changing the surface properties. Examples of surface modification of polymeric microrobots include chemical functionalization with metal layers<sup>[82,83]</sup> or metal nanoparticles,<sup>[84]</sup> via biotin-streptavidin interactions,<sup>[85]</sup> or using photoinitiators.<sup>[86]</sup> Selective metallization is also possible by electron beam physical vapor deposition through a mask which is 3D printed together with the microrobot.<sup>[63,87]</sup>

Interestingly, DLW enables *4D microprinting*, i.e., 3D printing of adaptive and dynamic microstructures.<sup>[88–91]</sup> Naturally, DLW of functional materials is challenging, but nevertheless achievable.<sup>[92]</sup> 2PP fabrication of multimaterial structures is another important challenge. Few multimaterial structures fabricated by 2PP have been reported to date, and they either relied on sequential fabrication steps. Ideally, multimaterial structures could be fabricated using a single multicomponent photoresist for which different excitation wavelengths trigger the selective crosslinking of its components.<sup>[92]</sup> Alternatively, a microfluidic platform that enables a multistep automatic procedure was reported for multimaterial DLW.<sup>[35]</sup>

Nanoporous polymeric structures were also demonstrated, using a 2PP process exploiting phase separation between the polymerizable photoresist component pentaerythritol triacrylate (PETA) and acetates with long hydrocarbon chains used as porogen.<sup>[93]</sup>

Another noteworthy approach in DLW is *write-and-erase*, pioneered by Wegener and coworkers.<sup>[94–96]</sup> After the DLW of carefully engineered polymer precursors, selective cleavage of the solid polymeric microstructures can be induced chemically<sup>[94,95]</sup> or by using a wavelength different from that of the laser exposure process.<sup>[96]</sup>

A fascinating perspective for in vivo applications requiring cleavable polymers is the fabrication of biodegradable polymeric structures. A home-made mixture containing poly(ethylene glycol) diacrylate (PEGDA) 575, PETA and the Irgacure-369 photoinitiator was used for 2PP DLW, after which the degradation of the crosslinked structures was observed over 36 h upon incubation in 0.01 M NaOH at 37 °C in 5% CO<sub>2</sub> with >80% humidity.<sup>[18]</sup> Another example of biodegradable 3D-printed structures came from Nelson and coworkers, who developed soft, and enzyme-degradable microrobots.<sup>[97]</sup> The hydrogel microrobots were fabricated using biocompatible gelatin methacryloyl (GelMA) and subsequently degraded, either using solutions of the enzyme collagenase, or by cell-secreted proteases, suggesting that this approach is particularly suitable for in vivo applications. Recently, multimaterial microstructures fabricated by DLW were selectively dissolved by the digestive enzyme chymotrypsin.<sup>[98]</sup> Although these examples of biodegradable polymeric microrobots were actuated using magnetic forces, the concepts can be directly translated to light-controlled microrobots.

In addition to the photoresist selection and printing parameters' optimization, postprocessing of 2PP 3D-printed structures can contribute to achieving the desired material properties. For example, postprint curing can help improve the mechanical properties of hard polymers by increasing the degree of crosslinking,<sup>[99,100]</sup> thermal reflow can reduce surface roughness for fast printed structures,<sup>[101]</sup> and isotropic plasma

etching and/or pyrolysis can be used to improve the resolution beyond 100 nm.<sup>[102]</sup>

### 3. Light-Powered Microrobots—Types and Examples

#### 3.1. 3D-Printed Hard Polymeric Microrobots

3D-printed polymeric microrobots controlled by focused light beams have been around for nearly two decades.<sup>[2]</sup> A plurality of commercial acrylic or epoxy-based negative photoresists,<sup>[85,87,103–106]</sup> as well as the hybrid organic–inorganic materialOrmocomp,<sup>[107]</sup> are used for 2PP DLW of hard polymeric microrobots. The hard polymeric microrobots covered by this section do not exhibit any shape-morphing properties, and instead their shape is defined during the fabrication process and remains unchanged during actuation.

The stiffness of polyacrylate-based 2PP 3D-printed structures has been shown to have higher values at higher degrees of conversion.<sup>[108]</sup> The Young modulus for such microstructures ranges from a few MPa to several thousand MPa and follows a quadratic relationship with density.<sup>[99]</sup>

Another optical manipulation approach is to induce rotation in the microrobots by applying torque through focused laser beams.<sup>[103,104]</sup> Finally, microrobots with metallized components can be exploited for thermoplasmonic effects upon laser illumination.<sup>[63,87]</sup>

Selected examples of 3D-printed hard polymer microrobots are shown in **Figure 5**. Köhler et al. nicely demonstrated how precise both 2PP and optical trapping are for the micromanipulation of an optical screw-wrench.<sup>[106]</sup> They 3D-printed three components for a microrotor—a screw, a rotor, and a nut—and used HOT to assemble the components (Figure 5A), and induce rotation of the microrotor. Optical trapping enabled the positioning and screwing of the rotor and nut, and was additionally used to apply torque on the microrotor.

Simpson's group developed optically actuated surface scanning probe microrobots.<sup>[105,109]</sup> Some of their designs are shown in Figure 5C, including the position of the optical traps and tracking points employed while scanning the surface.

Control of living cells has always been one of the main goals of optical manipulation. Although nIR is generally considered safe for manipulating biological entities, the risk for photodamage can be further reduced using indirect manipulation, which is desirable for particularly sensitive or rare cells.<sup>[19,110]</sup> Therefore, a number of microrobots for indirect manipulation have been reported, including the first articulated light-powered microrobot (Figure 5C),<sup>[70]</sup> a multiple microrotor system for hydrodynamic manipulation (Figure 5D),<sup>[111]</sup> microrobotic grippers that can, in pairs, grab, and transport cells to a desired location (Figure 5E),<sup>[19]</sup> and linear microrobots that can, also in pairs, either push or rotate filamentous cells.<sup>[112]</sup> As another cell-related application, Kelemen's group recently reported microrobots for single-cell elasticity measurements (Figure 5F).<sup>[113]</sup>

On the other hand, thermoplasmonic effects inducing fluid flow changes have been exploited to, e.g., load and unload a hollow-body syringe microrobot,<sup>[87]</sup> or to create a natural convection flow in a closed microfluidic channel.<sup>[63]</sup> Figure 5G shows an

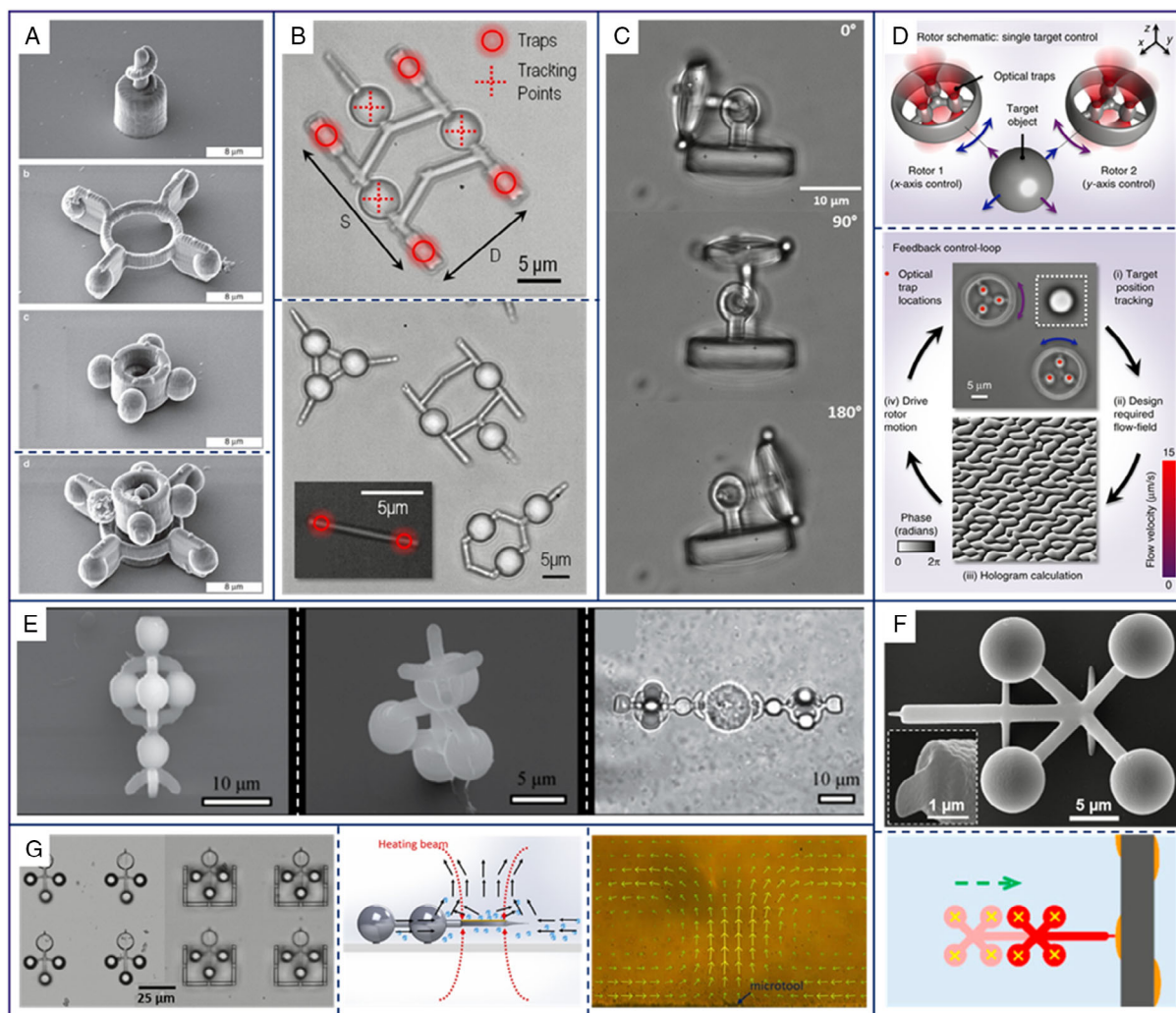


**Figure 5.** Examples of 3D-printed hard polymeric microrobots. A) Scanning electron micrographs of the individual components of a microrotor, and (bottom) assembled microsystem for microfluidic applications. Reproduced under the terms of the CC-BY license.<sup>[106]</sup> Copyright 2017, The Authors, published by Springer Nature. B) Ultralow force surface scanning probe for characterizing the topology of sensitive samples. Optical traps are used to displace the probe on a surface and the position of the tracking spheres is analyzed and used to compute sample topology. The scanning electron micrographs show (top) the position of traps and tracking points, and (bottom) different surface scanning probe microrobot designs. Reproduced with permission.<sup>[109]</sup> Copyright 2012, Optical Society of America. C) Articulated microrobot for indirect cellular manipulation. The three images show the rotation of the microrobot's mobile head. Reproduced with permission.<sup>[70]</sup> Copyright 2017, Wiley-VCH GmbH. D) Microrotors for indirect optical trapping and hydrodynamic manipulation. Schematic representation of the (top) principle for single target control and (bottom) key steps in the feedback control loop. Reproduced under the terms of the CC-BY license.<sup>[111]</sup> Copyright 2019, The Authors, published by Springer Nature. E) Microrobots equipped with fork-like clamps for indirect cell manipulation. (Left, middle) Scanning electron micrographs of the microrobot. (Right) Image of two microrobots transporting a single cell. Reproduced under the terms of the CC-BY license.<sup>[19]</sup> Copyright 2020, The Authors, published by MDPI. F) Microrobots for cell indentation experiments. (Top) Micrograph of a single microrobot, with an inset showing its tip. (Bottom) Schematic representation of the cell indentation experiment. Reproduced under the terms of the CC-BY license.<sup>[113]</sup> Copyright 2020, The Authors, published by MDPI. G) Microrobot equipped with a thermoplasmonic disk for mixing in microfluidic channels. (Left) Images of 3D-printed microrobots without and with the mask for selective metallization. (Middle) Schematic of the thermoplasmonic effect. (Right) Natural convection flow pattern induced by a microrobot upon illumination of its gold-coated disk. Reproduced with permission.<sup>[63]</sup> Copyright 2018, Optical Society of America.

array of polymeric disk microrobots, both with and without the mask for selective gold physical vapor deposition, together with the schematic representation of the thermoplasmonic effect generated upon illumination of the gold-coated disk, and the natural convection flow pattern observed by actuating the microrobot in a closed microfluidic channel.<sup>[63]</sup> In these examples,

light has a dual function: i) power source for microrobot motion, which is achieved through optical trapping, and ii) actuator enabling thermoplasmonic effects through off-resonance excitation of the surface plasmons of gold.

In addition to the examples shown in Figure 5, researchers have been exploring a number of different applications for

light-powered hard polymeric microrobots. In recent years, microrobotic waveguides,<sup>[114]</sup> microrobots with a segment covered by silver nanoparticles for surface-enhanced Raman scattering studies,<sup>[83]</sup> microrobotic microsnap fits for cantilevers,<sup>[107]</sup> and microrobotic dumbbells for fluid viscosity characterization<sup>[115]</sup> were reported.

The flexibility in 3D design, coupled with the excellent control accuracy, recommends 3D-printed hard polymer microrobots controlled by optical trapping for applications where precision is the key element.

### 3.2. Light-Responsive Microrobots with Soft Bodies

The use of softer polymeric materials with smart behavior represents another opportunity for the development of light-driven microrobots.<sup>[116–118]</sup> Unlike the hard polymeric microrobots discussed in Section 3.1., which have predefined and rigid shapes, soft microrobots are based on smart materials able to adapt their shape in response to a specific environmental cue. The soft nature of such materials strongly depends on the formulation. Typical Young modulus values range from tens of kPa for hydrogels<sup>[119]</sup> to MPa for liquid crystalline networks (LCNs).<sup>[120]</sup> To the best of our knowledge, the Young modulus values for such materials prepared by 2PP DLW have not yet been investigated, and might be significantly different from those measured at the macroscale. Such materials are ideal for constructing microrobots which mimic many of the functional properties of biological tissues or microorganisms.<sup>[121]</sup> In this class of microrobots, light works only as energy fuel, whereas the microrobot bodies perform the real mechanical action, from gripping to movement, through dynamic shape morphing.

For fabricating soft light-responsive microrobots, two classes of polymers are most commonly used: hydrogels and liquid crystalline polymers.<sup>[122]</sup> **Figure 6** shows examples of light-powered soft microrobots fabricated using such polymers.

#### 3.2.1. Hydrogels as Light-Controlled Microrobot Materials

Hydrogels are hydrophilic networks able to contain high amounts of water. In microrobotics, and especially for microrobots that move and perform tasks in liquid environments, chemically crosslinked hydrogels are of great interest. Using thermoresponsive polymers, such as poly(*N*-isopropylacrylamide) (PNIPAm), it is possible to achieve a shape change by modulating the swelling degree of the material. PNIPAm has a low critical solution temperature, around 32–34 °C, whereas above these temperatures, the network collapses, reducing its volume by water deswelling.<sup>[123]</sup> This shape change is spatially isotropic and entirely reversible upon cooling.

To achieve a specific microrobotic operation, different methodologies to control or direct the deformation of shape-changing materials have been adopted. A first example is exploited for the microgripper shown in **Figure 6A**.<sup>[124]</sup> This venus flytrap-like structure is based on a polymeric bilayer, where a PNIPAm layer is coupled with a non-thermo-responsive hydrogel prepared from polyethylene glycol diacrylate. The microgripper is fabricated through a two-step process involving photolithography. Due to the different swelling capabilities of the two component

materials, the structure closes under water and can be opened by heating up to 40 °C due to PNIPAm deswelling. Doping the responsive layer with graphene oxide particles enables control over the gripper shape by means of nIR light. Irradiation by a 785 nm laser allows controlled hydrogel heating thanks to dissipative effects with complete deswelling in a subminute time scale. Thus, the gripper can be opened by light to release a cargo stored inside the closed form.<sup>[124]</sup>

Extending this concept to movement in liquids, as desired in the case of swimming microrobots, requires a careful design, because different physical laws govern this action at the micro-/nanoscale than in the macroscopic world. At the micro-metric scale, adhesion and viscous forces predominate over other forces. Therefore, special strategies—already exploited by natural microorganisms—have to be adopted to achieve a net movement. As explained by Purcell in the so-called “scallop-theorem,” swimming requires a series of movements that are nonreciprocal at low Reynolds numbers.<sup>[125]</sup> The body deformations have to follow a pathway with a different space/time dependence on the forward and shape recovery actions. Taking again inspiration from nature, the two main mechanisms for swimming at the microscale are the rotation of helical flagella or the beating of cilia.

Möller and coworkers proposed how to reproduce both flagella and cilia by exploiting light-responsive hydrogels, in particular, by combining bilayer compositions with asymmetric swelling of the PNIPAm layer.<sup>[126]</sup> The hydrogel doped with gold nanoparticles achieved a material heating with a thermal jump of more than 20 °C in millisecond time upon irradiation with an nIR laser. Light irradiation with short pulses can in this case be used to introduce asymmetry in the otherwise isotropic deswelling process thanks to nonequilibrium conditions, where the temperature changes faster than the volume, thus creating asymmetry in the shape deformation as shown in **Figure 6B**. Moreover, sputtering of the 2D printed microstructures with a rigid gold “skin” enabled the preparation of different 3D shapes. Depending on the geometrical parameters (e.g., the thickness of PNIPAm and gold layers), spiral, helix, or hollow-tube 3D structures can be prepared starting from the same 2D hydrogel microstructures.<sup>[126]</sup> The 3D microstructures shown in **Figure 6B** were obtained starting from layered 2D microstructures fabricated by photolithography.<sup>[126,127]</sup> The helical structure shown in **Figure 6B** was irradiated for 80 ms, causing its unwind and then a change in twisting handedness. The whole deformation/recovery process presented nonreciprocity in both the evolution of length and the diameter of the spiral. By changing the irradiation sequence to 16/20 ms on/off, the helix was able to rotate along an axis normal to its long axis. When placed in a confined environment, such as in between two glass surfaces, directional motion displacement was obtained, as shown in **Figure 6C**.<sup>[127]</sup> This approach is very appealing for motion and manipulation in microfluidic channels, which are ubiquitous in lab-on-a-chip devices that are attracting more and more attention for different applications.

Using a similar approach, a light-driven rotor based on a photoresponsive 2D spiral attached to a microsphere was described.<sup>[128]</sup> Under pulsed irradiation, the system was able to rotate thanks to nonreciprocal curling deformations of the spiral tail. Changing the irradiation conditions (e.g., duration of pulses, power), the kinematics of the curling deformation



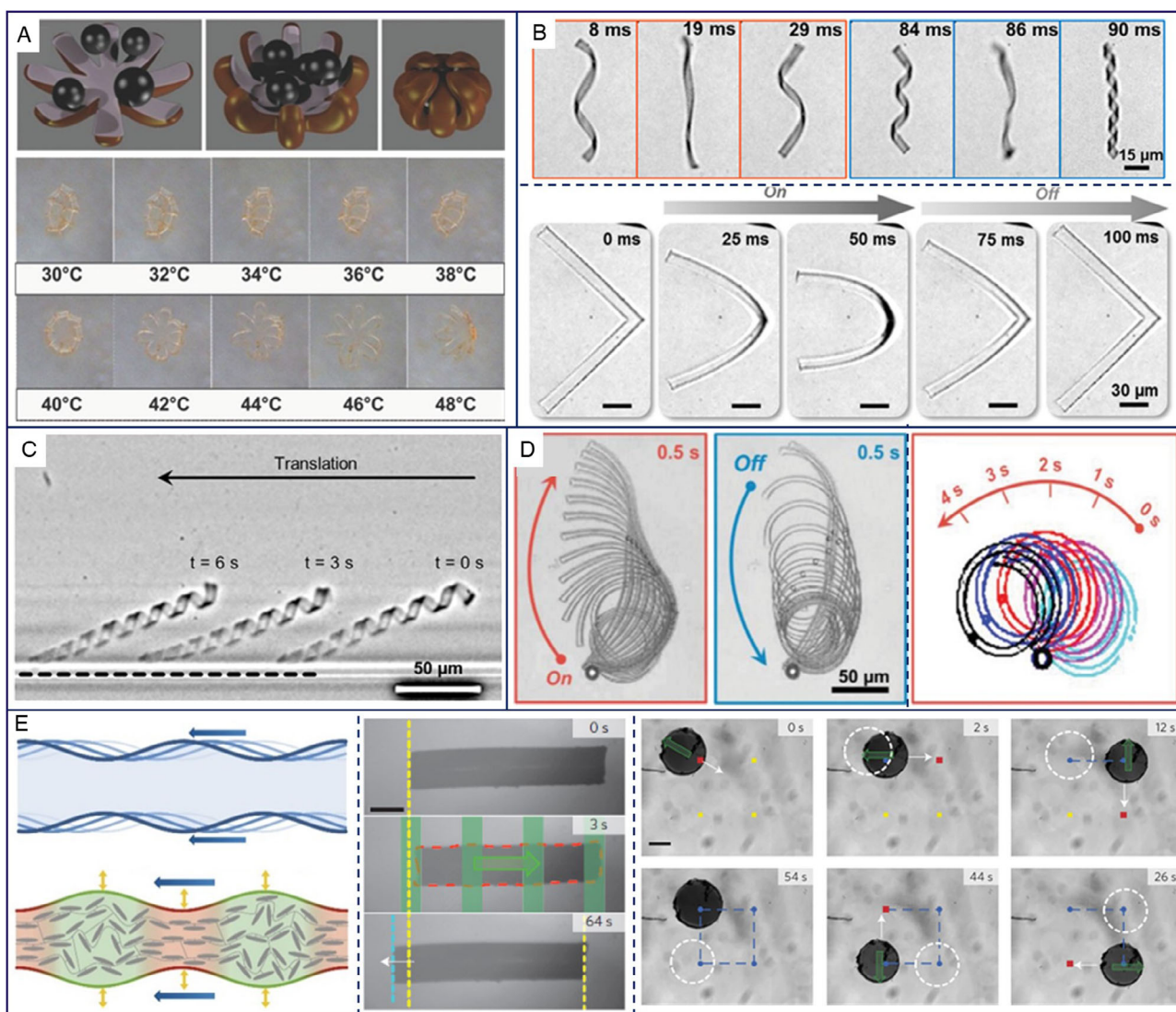


**Figure 6.** Examples of soft microrobots prepared using smart materials. A) A hydrogel microgripper. Schematic representation of the gripping principle and optical images of its unfolding under heating up to 48 °C. Reproduced with permission.<sup>[124]</sup> Copyright 2013, Wiley-VCH GmbH. B) Photothermal actuation in hydrogel microstructures by a nonequilibrium process: (Top) A helix prepared by irradiating a bilayer hydrogel-gold skin structure for 80 ms. Reproduced with permission.<sup>[126]</sup> Copyright 2017, American Chemical Society. (Bottom) A 2D V-shape PNIPAm structure irradiated for 50 ms. After only 30 ms, the helical chiral structure is reverted. Reproduced with permission.<sup>[127]</sup> Copyright 2017, The Authors, published by Wiley-VCH GmbH. C) Directional movement of an oscillating helix hydrogel-based microstructure confined between two glass surfaces. Reproduced with permission.<sup>[127]</sup> Copyright 2017, The Authors, published by Wiley-VCH GmbH. D) (Left) Superimposed images of a spiral rotor under irradiation for 0.5 s and relaxation for 0.5 s and (right) superimposition of the thresholded outline of the rotor at different times. Reproduced under the terms of the CC-BY license.<sup>[128]</sup> Copyright 2019, The Authors, published by Wiley-VCH GmbH. E) LCN-based swimmer microrobots. (Left) Schematic illustration of the bioinspired worm-like travelling wave deformation shape change occurring during homogeneous phase transition or illumination with a patterned light. (Middle, right) Optical images of a microtube displacement under travelling patterned irradiation. (Middle) Green overlays, direction according to green arrows, yellow dashed line is the reference position. (Right) Optical microscopy images of a microdisk locomotion along a square path—the travelling wave direction is indicated by the green arrows, and the disk's direction of travel to the next waypoint by the white arrows. Reproduced with permission.<sup>[134]</sup> Copyright 2016, Springer Nature.

can be adjusted to obtain bending and unbending cycles that follow distinct paths. This system mimicking natural cilia is shown in Figure 6D and satisfies the requirement for net rotational thrust at low Reynolds numbers.<sup>[128]</sup>

A different yet interesting case is that of crawling robots, where a reciprocal actuation, such as a simple contraction–

expansion cycle, was shown to lead to efficient movement by exploiting a head-to-tail asymmetry of the surface friction on ratchet surfaces.<sup>[129]</sup> Microrobotic crawlers prepared by using photoresponsive PNIPAm with embedded gold nanoparticles arranged in a simple shape with a size of  $100 \times 50 \times 30 \mu\text{m}^3$  produce, when irradiated on one side, a contraction–expansion cycle

that results in a net displacement due to the hysteresis of the cycle of friction with the surface during the whole deformation process. The movement is parallel to the line connecting the irradiation spot and the robot center of mass, which allows for control over the crawling direction. This concept was also demonstrated for a U-shaped microrobot that can be steered in the movement plane by irradiating one of its rectangular elements, or can undergo straight movement upon simultaneous irradiation of both ends.<sup>[129]</sup>

### 3.2.2. Liquid Crystalline Polymers as Light-Controlled Microrobot Materials

Another class of promising soft materials for light-driven microbotics are liquid crystalline elastomers (LCEs) and LCNs.<sup>[130–133]</sup> These polymers are prepared by grafting liquid crystal (LC) moieties (mesogens) inside a polymeric network, which leads to an anisotropic molecular structure of the whole system. In response to stimuli such as heating, the molecular order is gradually lost, leading to a progressive deformation of the whole material. In particular, a contraction along the liquid crystalline alignment direction and an expansion in the perpendicular direction are observed.<sup>[131]</sup> A schematic example of the shape-change in LCN is shown in Figure 6E.<sup>[134]</sup> Some remarkable features of this behavior are the reversibility of the movement once the stimulus is removed, and the possibility to program different deformations by playing solely with the LC alignment.<sup>[133,135]</sup> Bilayer structures or crosslinking gradients are not required to obtain out of plane movements. In contrast to hydrogels, LCNs can work in environments in addition to water, as deformation can take place in other solvents, and LC alignment engineering can easily lead to bending, torsional, or rotational movement.<sup>[136]</sup>

Various bioinspired light-sensitive robots based on light-sensitive LCE, with dimensions in the millimeter-to-centimeter scale, have been described.<sup>[137,138]</sup> Approaching the micrometer scale and producing LCE-based microrobots is much less common, likely due to challenges in the material actuation at the smaller scale. Palagi et al. exploited LCNs prepared by photopolymerization of acrylate-based mesogens to fabricate different swimming microrobots.<sup>[134]</sup> The basic concept to obtain nonreciprocal motions was to induce a travelling wave deformation in the microrobotic bodies by actuating them with a dynamic light pattern. The LCN was doped with an azodye able to cause heating of the material up to 100 °C depending on the power density.<sup>[59]</sup> Selective irradiation of target parts of the LCN lead to asymmetric deformation. By scanning the projected light, the travelling deformation allowed for microrobot swimming. Figure 6E shows the movement of two different microstructures exploiting this methodology, a LCN cylinder prepared by manual fiber drawing,<sup>[139]</sup> and a microdisk fabricated using photolithography.<sup>[134]</sup> The microdisk can swim following different 2D pathways, and multiple swimmers can be controlled simultaneously using a simple optical setup including a SLM.

All the examples presented in this section are based on 2D structures prepared as building blocks by standard lithographic techniques, while a real 3D structuration has not yet been exploited for operation in liquid. Nevertheless, true 3D soft microrobots are expected to emerge in the near future, as recent

studies demonstrated DLW for both hydrogels and LCN. In case of hydrogels, asymmetric motions have been obtained by playing on different swelling degrees created inside the same structure using different writing powers, which create different polymerization degrees.<sup>[61,89]</sup> In the case of LCN, the monomeric mixture was first aligned in a standard LC cell and then polymerized to obtain microstructures with a deformation that is determined by the molecular order already present before the writing step.<sup>[140,141]</sup> LC cells presenting multiple alignments can be used to obtain different motions in selected parts of a single microstructure.<sup>[142]</sup>

For LCN, DLW has already been used to create light-powered microrobots operating in air, where both walking robots<sup>[62]</sup> and grippers.<sup>[143]</sup> have been demonstrated. The walker microrobot was printed to have a LCN body combined with four rigid conical legs which reduce the interaction with the surface and thus the adhesion force. Under chopped light, the cyclic body contraction allowed step-by-step movement of the microrobot on a glass surface.<sup>[62]</sup> To obtain a microgripper, a simple star-shape LCN structure incorporating different LC alignments was prepared. Upon actuation, the bending of the different parts toward the same central point was achieved, thus mimicking the basic gripping operation of a human hand. In this manner, the manipulation of microblocks made from different materials was demonstrated.<sup>[143]</sup>

These examples demonstrate the feasibility of both combining materials with different properties and of the use of multiple LC alignment to achieve asymmetric deformation in the same platform thanks to multistep writing processes. The speed and extent of contraction under light or heating can be tailored by different strategies, such as modulating the crosslinking agent content in the monomer mixture,<sup>[144]</sup> increasing the flexible spacer of the mesogens to enhance material flexibility,<sup>[145]</sup> or playing on DLW fabrication parameters to achieve different polymerization degrees.<sup>[89]</sup>

### 3.3. Nonpolymeric Light-Powered Microrobots

The objects discussed herein generally have much simpler shapes than their 3D-printed counterparts, and thus the term microrobot applies very loosely to most examples. Instead, most of them are either very simple particles actuated in innovative ways, or Janus particles, i.e., asymmetrical structures with two distinct types of physicochemical properties,<sup>[146]</sup> with response to light. Motion often also relies on different principles and not on optical trapping, but light always acts as an actuator for the intended application.

In 2011, Swartzlander et al. demonstrated a stable optical lift for the optical manipulation of a semicylindrical rod fabricated by photolithography in the OIR 620 photoresist.<sup>[147]</sup> The optical lift performed well only for cambered refractive rods. This represents an interesting demonstration of optical manipulation of microrobots that does not involve direct optical trapping. Two years later, semicylindrical and trapezoidal refractive optical wing oscillators with reflective back surfaces were reported.<sup>[148]</sup> These optical wings experienced both lift and torque upon quasi-uniform illumination.

Birefringent vaterite particles controlled by light were used to direct axon growth in a neural cell culture.<sup>[149]</sup> By simply

changing the illumination from linearly polarized to circularly polarized light, the resultant optical angular momentum causes the birefringent particles to spin in controlled manner, which was exploited to induce axon growth directionality. Similarly, optical forces were harvested to induce motion in gold nanorod plasmonic microrobots.<sup>[150]</sup> In this case, control can be achieved either by rotating the laser polarization, or through transfer of photon spin angular momentum or orbital angular momentum. In addition to acting as driving force, light induces photothermal effects in plasmonic microrobots, which can be of interest for certain applications.

Typically, nonpolymeric light-driven microrobots rely on object asymmetry, either in terms of shape, or of physicochemical properties. However, the limited penetration depth of light in liquid environments was exploited to induce controlled motion of isotropic titania (TiO<sub>2</sub>) microspheres.<sup>[151]</sup> The semiconductor microrobots were shown to exhibit phototactic behaviors inspired from naturally occurring microorganisms. The system asymmetry necessary for controlled motion was ensured by selecting the illumination direction, whereas the microrobot isotropy was conducive to a behavior less dependent on rotational

Brownian diffusion or local flows compared with the case of using Janus particles.

Figure 7 shows examples of light-powered nonpolymeric microrobots. The structures shown in Figure 7A–C are photocatalytic microrobots, which make use of chemical reactions catalyzed by UV light. The TiO<sub>2</sub>/Au/Mg microrobots developed by Li et al. (Figure 7A) self-propel in chlorinated aqueous media and can degrade pollutants upon UV irradiation.<sup>[51]</sup> In a similar manner, Au/Ni/TiO<sub>2</sub> Janus microrobots reported by Wang et al. self-propel in H<sub>2</sub>O<sub>2</sub> when irradiated with UV light and can capture polystyrene particles by phoretic interactions.<sup>[21]</sup> Another significant example of photocatalytic microrobots able to clean the liquid environment from selected components are fuel-free brush-shaped ZnO-based microstructures. The microrobots exhibit directional motion upon UV exposure and can help degrade nitroaromatic explosives,<sup>[152]</sup> or perovskite-like Bi<sub>2</sub>WO<sub>6</sub> microrobots can destroy textile fibers upon visible light photoactivation.<sup>[153]</sup> Recently, Zn/Au Janus rods propelled by H<sub>2</sub>O<sub>2</sub> which can switch from ballistic to rotational motion upon UV irradiation (Figure 7B) were reported.<sup>[154]</sup> In a more environmentally friendly approach, bismuth oxyiodide/Au Janus microrobots (Figure 7C)

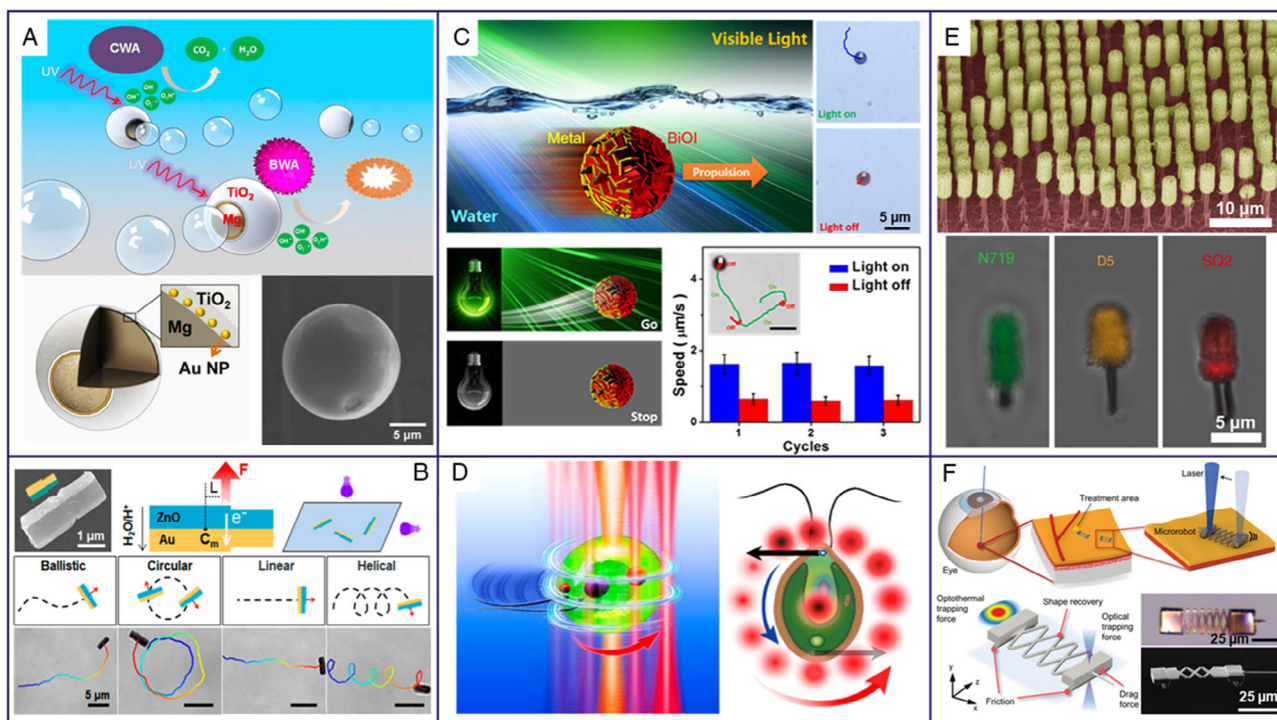


**Figure 7.** Examples of light-powered nonpolymeric hard microrobots. A) Water-driven spherical TiO<sub>2</sub>/Au/Mg microrobots for photocatalytic degradation of toxic chemicals. (Top) Process schematic (bottom left) microrobot structure, and (bottom right) scanning electron micrograph. Reproduced with permission.<sup>[51]</sup> Copyright 2014, American Chemical Society. B) ZnO/Au Janus rod microrobots propelled by H<sub>2</sub>O<sub>2</sub> when activated by UV light: single microrobot, process schematic, and motion modes. Reproduced with permission.<sup>[154]</sup> Copyright 2020, American Chemical Society. C) Visible light-driven bismuth oxyiodide Janus microrobots. (Top) Process schematic and (bottom) response to light. Reproduced with permission.<sup>[155]</sup> Copyright 2017, American Chemical Society. D) Schematic of the optical actuation of *Chlamydomonas reinhardtii* living microrobots, (left) side view and (right) top view. The central beam corresponds to the stable optical trap, while the surrounding red beams show the annular scanning optical trap sequence. Reproduced with permission.<sup>[157]</sup> Copyright 2020, American Chemical Society. E) Dye-sensitized Janus nanotree microrobots driven by visible light. (Top) false-colored scanning electron micrograph and (bottom) confocal microscopy fluorescence mapping of dye loading into the microrobots. Reproduced under the terms of the CC-BY license.<sup>[64]</sup> Copyright 2017, The Authors, published by Springer Nature. F) Ni–Ti shape memory alloy microrobot for intraocular surgery. (Top) Process schematic (bottom left) actuation schematic, and (bottom right) images showing the microrobot. Reproduced with permission.<sup>[158]</sup> Copyright 2019, Wiley-VCH GmbH.

propelled by water upon visible light activation were developed.<sup>[155]</sup> CoO/TiO<sub>2</sub> photocatalytic microrobots with magnetic properties were engineered to respond to a wide range of wavelengths, from UV to nIR, and their direction could be controlled by changing the actuation wavelength.<sup>[156]</sup>

A biological microrobot used for indirect manipulation in complex media is shown in Figure 7D.<sup>[157]</sup> The living microrobots consist simply in biflagellate *Chlamydomonas reinhardtii* freshwater microalgae manipulated by a stable optical trap and an annular scanning optical trap which induces controlled rotation and motion.<sup>[157]</sup>

Figure 7E shows the TiO<sub>2</sub>/Si nanotree Janus microrobots developed by Zheng et al.<sup>[64]</sup> Upon incorporating different dyes in the nanotree microrobots, the authors were able to independently control individual microrobots by stimulating them with different wavelengths.

A nature-inspired biomedical microrobot fabricated in a Ni–Ti shape memory alloy is shown in Figure 7F.<sup>[158]</sup> The metallic structure was fabricated by focused ion beam milling and mimics shrimp locomotion upon laser actuation. Its propulsion is driven by optothermal trapping forces induced by the thermophoretic response of the Ni–Ti shape memory alloy.

Recently, plasmonic linear microrobots were demonstrated.<sup>[159]</sup> The microrobots consisted of asymmetric nanostructure pairs embedded in silica microblocks and were fabricated using a combination of electron beam lithography and dry etching. The gold-coated components included allowed for plasmon-based responses of the microrobots. Linear motion was demonstrated using linearly polarized light with a wavelength of 910 nm and an intensity of 0.4 mW μm<sup>-2</sup>. By tailoring the microrobot design, a rotation motion was also demonstrated.

Although such objects are definitely noteworthy, they will not be further discussed in other sections, which refer exclusively to polymeric microrobots. Interested readers are instead directed to a review article focused on various types of light-driven microrobots.<sup>[160]</sup>

## 4. Challenges in the Fabrication and Optical Actuation of Polymeric Microrobots

For light-powered microrobots, two main categories of challenges can be highlighted, one related to the fabrication, and the other to the optical control of the microrobots. Furthermore, different types of aspects need to be considered for real-world applications, such as the microrobot biocompatibility and long-term biosafety, or the imaging and tracking of the microrobots while they are carrying out their tasks in a complex environment. While a number of these challenges are common for hard and soft polymeric microrobots, others are specific to only one of these types, as discussed in the following sections.

Furthermore, two significant challenges encompassing both fabrication and actuation should be mentioned. The first such challenge is scalability. For 2PP 3D printing, the microrobot fabrication time directly increases with the number of microrobots due to the serial nature of the fabrication process. In contrast, photolithographic fabrication of soft microrobots can be upscaled more easily. On the other hand, nowadays, optical control is also often limited to a relatively small number of microrobots, as

dictated by the characteristics of the optical manipulation setup. The second challenge is that of user-friendly manipulation. Currently, fabrication and manipulation of light-powered microrobots often requires an interdisciplinary team of highly trained researchers. To become truly useful outside a laboratory environment, microrobots need to be fabricated on a much larger scale, and they need to be either autonomous, or easy to control. This is further discussed in Section 5.

### 4.1. Fabrication

There are several fabrication-related challenges for both soft and hard light-powered microrobots. The first issue is related to the microrobot size. Hard microrobots can in principle be micrometer- or even nanometer-sized, as optical trapping of such small structures is achievable.<sup>[58]</sup> However, the 3D printing resolution becomes a critical parameter in this case, for both the trapping handles and task-related microrobot features. **Figure 8** shows examples of such challenges. The disk-tip microrobot shown in Figure 8A was designed to include a syringe-like tip, shown in Figure 8B, with a diameter of 200 nm at the apex and a length of 2 μm. In practice, however, although the 200 nm diameter was achieved, the length was only around 500 nm, 4 times less than in the design. On the other hand, shrinking the microrobot implies the use of smaller trapping handles. Figure 8C shows a 3D-printed sphere with a diameter of 6 μm fabricated using the IP-L 780 photoresist. Despite using a photoresist optimized for high resolution, the individual print voxels are clearly observable at this scale, and the surface roughness is quite high, which might interfere with the efficiency of optical trapping and manipulation. If printing very small microrobots is highly desirable, the photoresist and 3D printing parameters require careful optimization. In addition, post-processing techniques, briefly described in Section 2.2., should be applied to further improve the resolution and overall quality of the printed structures.

In the case of soft microrobots, in addition to the resolution dictated by the adopted lithographic techniques, the minimal size is governed by the required physical dimensions of the different parts of the robot that allow accomplishing a certain task. This becomes immediately clear if you think of a bending robot arm that should grasp a microscopic object. In this case, the curvature radius that the microrobot should form is constrained by the object dimension, coupled with the material's ability to deform. Indeed, shape-changing materials can bend, twist, or contract to a certain extent with respect to their dimension (e.g., contractions up to 50% for LCE). Moreover, the generated force should be sufficiently large to overcome the adhesive forces, in the case of dry-environment living microrobots, or the viscous forces, for microrobots actuated in liquids. To this end, the smallest walking microrobot, 60 μm in length, has been demonstrated to walk on rough and smooth surfaces overcoming friction forces.<sup>[62]</sup> Both the design of its legs with a sharp rigid tip to limit adhesive forces, and the elastic light-responsive body able to contract up to 20% of its total length at 50 Hz, contributed to the microrobot's ability to walk when powered by light.

In fluids, the balance between inertial and viscous forces, whose ratio is called the Reynolds number, is crucial. At low Reynolds number, where inertia has a negligible contribution,

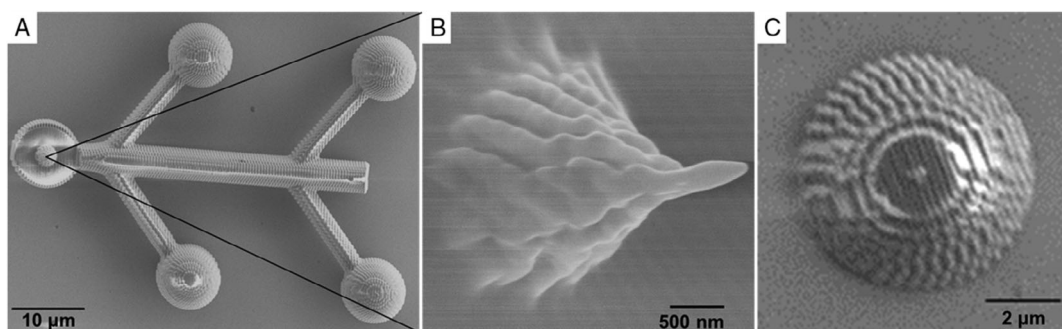


**Figure 8.** Scanning electron micrographs. A) 3D-printed disk-tip microrobot top-view and B) zoom-in on the tip feature acquired using a 30° stage tilt. Reproduced with permission.<sup>[208]</sup> Copyright 2018, Society of Photo-Optical Instrumentation Engineers. C) 3D-printed IP-L 780 microsphere with a diameter of 6 μm where the print lines and layers are clearly observable.

swimming at the microscale requires a nonreciprocal motion, i.e., motion not being time-reversed because of the time-independence of the linear Stokes equation. This should be pursued using a tailored geometrical design and/or material engineering, using, e.g., polymers with different time responses for the various moving parts, structures with different spectral responses in combination with multicolor illumination, or multimaterial microstructures. An interesting example of multimaterial use in DLW for developing microrobots was recently reported by Ma et al., who modified a hard SU-8 *microskeleton* with a pH-responsive protein, bovine serum albumin (BSA), acting as *contracting muscle*.<sup>[161]</sup> Whereas the musculoskeletal microrobots thus fabricated were actuated by pH changes, the approach could be adapted to light-powered microrobots by replacing the pH-responsive component with a light-responsive material.

A further advance in swimming strategies will be the control of the forward and backward propulsion. This has recently been demonstrated in magnetic microrobots containing two magnetized spirals of opposite handedness. The competition between the two spirals can be tuned by applying a magnetic field within a given band of frequencies for controlling the positive or negative advancement of the microrobots in microfluidic channels.<sup>[162]</sup> In the case of light-powered microrobots, the same principle could be obtained using microrobots whose different parts are controlled by different wavelengths. By combining materials doped with dyes that have complementary absorption, color modulation can be introduced in the stimulus to control the movement asymmetry.<sup>[163]</sup> Control of forward and backward propulsion could be achieved by taking inspiration from a simple swimmer microrobot able to swim at low Reynolds numbers.<sup>[164]</sup> This microrobot consists of three spheres connected by two extendable bars of negligible thickness that sequentially elongate and contract in a nonreciprocal way.<sup>[164]</sup> Even more interestingly, a similar design with four spheres has been adopted as a case study to demonstrate that the locomotory gait can be optimized by reinforcement learning in terms of the displacement and depending on the environment, i.e., frictional or viscous fluid medium.<sup>[165]</sup> To this purpose, reinforcement learning<sup>[166]</sup> seems to outperform other machine learning approaches in designing adaptive locomotion strategies for microrobotic swimmers. Indeed, reinforcement learning is typically used for time-

evolving series of events and it rewards the success of an action with respect to the overall goal. This approach, already exploited for various macroscopic robots,<sup>[167]</sup> would fit nicely for the training of microrobots, as the dynamic and iterative learning process reproduces well the natural learning of living animals.

#### 4.2. Actuation

Achieving good optical control in complex samples is an important element in moving toward real-world applications. While optical manipulation and activation are very well established in water or nonscattering aqueous media, significant challenges occur in more complex media, such as biological or environmental samples.<sup>[58]</sup> These challenges apply to both hard and soft light-powered microrobots and are partly caused by the optical properties of complex media, among which turbidity and absorption are the most important, and are relevant to the control of both soft and hard light-powered microrobots. To overcome this, real-time phase manipulation through wavefront correction algorithms<sup>[168,169]</sup> or optical phase conjugation<sup>[170,171]</sup> seems particularly promising. However, the speed with which the system can be reconfigured is a critical element here. As turbid media are constantly changing, the phase needs to be readjusted accordingly to achieve and maintain good light focusing. Improvements in computational power and machine learning algorithms should help achieve suitable speeds in the near future. At present, there are a few machine learning models that optimize the locomotory gait to improve the swimmer speed,<sup>[172]</sup> or adapt to the environment,<sup>[173]</sup> but a practical demonstration is still lacking. Another option for wavefront engineering and thus improved light focusing in turbid media is the use of metasurfaces.<sup>[174,175]</sup> While metasurfaces enable device miniaturization, often show good performance, and are not subject to speed issues, they only allow for limited reconfigurability of the beam in the optical system they are integrated in.

In addition to real-time beam configuration, tailoring the trapped objects can improve their motion in complex media. For example, optical catapulting of polystyrene microspheres in mucus models shows a behavior that can be attributed to chemical interactions between the object and the medium.<sup>[176]</sup> It is expected that such interactions would play a role in the motion of microrobots in complex media with different

compositions. Tailoring the chemistry of the microrobots has been shown to confer stealth, nonimmunogenic or antifouling properties.<sup>[177]</sup> Another approach to enhance interface interactions is the use of micro- and nanoarchitectures inspired from nature. In a recent article, Li et al. demonstrated optical manipulation of a microrobotic rocket in the blood vessels of a mouse ear.<sup>[178]</sup> The microrobot rockets were designed based on the interface enhancement principle and included three micronozzles coated with a thin gold layer.<sup>[178]</sup> These examples show that both the shape and the chemical properties of the microrobots are important parameters to consider when it comes to improving motion in complex samples.

Regarding the challenge of light absorption in complex media, choosing a suitable wavelength where absorption is minimal is often sufficient, and can be complemented by an increase in the power used for optical manipulation, provided that the power increase does not cause additional issues with, e.g., biocompatibility. As mentioned in Section 2.1, the characteristics of the optical manipulation setup can pose challenges in terms of manipulation range, and microrobot observation. Due to the use of high NA objectives, HOT typically offer a freedom of less than 100  $\mu\text{m}$  on the Z-axis and 200–300  $\mu\text{m}$  in the XY plane, and only allow for top-view observation of the sample. The use of unconventional optical setups can help overcome these limitations.

Motion efficiency, defined as the mechanical power output divided by the overall energy input, is a fundamental aspect to consider. In the case of soft microrobots, a three-step energy conversion is necessary, as light first triggers a material response, which then in turn leads to microrobot motion. In azo-doped LCN, two different mechanisms of mechanical actuation can be identified. The dye molecule can absorb light and release energy into heat that thus induces the phase transition of the LCN or can exploit its isomerization, in between the *trans* and *cis* states to reorient the surrounding crosslinked networks. The two processes have two different time scales and energy efficiency and are determined by the nature of the photo-switch, considering its connection to the network (crosslinker or side-chain) and the life-time of the *cis* isomer.<sup>[179]</sup> Playing with the molecular formulation is thus possible to enhance the mechanical deformation efficiency of the light-responsive polymer. For an inchworm-like soft microrobot in both dry and wet environments, the best performance has been obtained by mean of crosslinker azobenzene moieties due to a constructive contribution between photochemical and photothermal effects in the actuation mechanism.<sup>[179]</sup> In the case of hard microrobots subjected to optical trapping, motion efficiency is generally higher, as the microrobot directly follows the path set by the optical traps. However, it is mandatory to ensure a suitable trap stiffness and trap displacement velocity in order for this to happen. The trap stiffness is influenced by a number of factors such as the characteristics of the optical setup (i.e., wavelength, NA of the objective, laser power), size of the trapped object, and difference in refractive index between the trapped material and its environment. The trap displacement velocity can easily adjusted be for individual experiments, so it is generally less critical.

Although light is an extremely flexible microrobot actuator, overcoming the challenges associated with optical manipulation in complex samples is not trivial. Furthermore, due to the low penetration depth of light in complex liquids and in tissues, it

is rather difficult to imagine microrobots with light as the only actuator operating in, e.g., the human intestine or at the bottom of a deep lake. The solution might be to supplement the use of light with that of an additional actuator among those described in Section 1. Magnetic control seems the most promising at the moment due to the magnetic field penetration depth which allows for in vivo actuation in a noninvasive and relatively safe manner. However, innovative technique combinations might prove even more auspicious for specific applications.

### 4.3. Biocompatibility

For some environmental applications, and most biomedical applications, biocompatibility is a critical element, which has been often overlooked in the early microrobot development studies. However, given the numerous potential applications of various types of microrobots for biomedical studies, biocompatibility has become more and more sought-after in recent years and important progress towards this goal has been made.<sup>[180]</sup> When aiming at real-world applications, the biocompatibility of the complete microrobot/actuation construct needs to be assessed. Of course, the use of biocompatible materials for fabrication is a key element of achieving biocompatibility, but it does not offer a biocompatibility “guarantee” for the microrobotic system.

Generally, a wide selection of biocompatible polymers is available. When commercial polymers are modified in-house, the biocompatibility of the final material should be characterized. Particular formulations of LCN have already been demonstrated to be biocompatible,<sup>[181]</sup> or even to favor the growth and maturation of cells in cultures.<sup>[182]</sup> Furthermore, the shape, size, and topology of microrobots might play an important role for overall biocompatibility. A recent study showed that to reduce potential inflammatory responses, the microrobot design should minimize any physical interactions with the cells of the immune system while improving the locomotion performance of the microrobots.<sup>[183]</sup>

Although light is generally considered to be an actuator suitable for biological applications,<sup>[184]</sup> a thorough biocompatibility study is necessary for each individual optical control configuration, as specific combinations of wavelength and power can have different effects on cells, tissues, or bodily fluids. Typically, nIR light is considered safe for biological entities, provided that the power used is not too high, as it is the case for optical trapping setups. To accomplish nIR actuation in photoresponsive LCN, one option is to use nIR dyes or nanoparticles to induce the photothermal mechanical response. Alternatively, recent works demonstrate the possibility to trigger the *trans* to *cis* azobenzene isomerization by nIR light.<sup>[60,61]</sup> Such approaches should be applied in the near future to expand the optical isothermal deformation to lower energy wavelengths, as opposed to the UV or blue light commonly used at the moment. In any case, assessing the effects of tailored optical actuation in model systems and target real-world systems is essential before unleashing the microrobots into the world.

### 4.4. In Vivo Imaging

Tracking of the microrobots in vivo is extremely important for biomedical applications. Different techniques can be used for

this purpose, such as optical tracking, magnetic imaging, X-ray imaging, ultrasound imaging, or fluorescence imaging. Each imaging modality has its specific requirements regarding both the microrobot characteristics and the instrumentation needed for imaging. Consequently, specific advantages and limitations can be associated with the use of each technique. A more elaborate description of the imaging modalities and their applications for biomedical microrobots can be found in a recent review article from Pané et al.<sup>[185]</sup>

Recently, an interesting approach based on structural colors was developed for identifying and tracking 3D-printed microrobots.<sup>[186]</sup> An identification and tracking segment was included in the microrobot body. The segment consisted of a micropattern displaying structural colors upon metallization. By changing the micropattern parameters, different structural colors could be obtained. In practice, this allowed observation through a microscope in a manner similar to fluorescence labeling, but the structural colors have the advantage that they do not bleach and do not require additional fabrication steps. The microrobots displaying structural colors were controlled by magnetic forces rather than using light, but the concept can be directly applied to light-controlled microrobots fabricated by DLW. Although this is a very interesting solution, it is yet unclear if it can be readily translated to *in vivo* experiments.

The light-controlled microrobot rockets reported by Li et al. were imaged using photoacoustic tomography in two types of biologically relevant samples, bovine blood, and an *ex vivo* mouse blood vessel covered by a mouse ear.<sup>[178]</sup> The presence of a gold skin around the microrobot body allowed for the amplification of the photoacoustic signal, resulting in good contrast in the biological samples (Figure 9).

## 5. Envisioned Applications

### 5.1. Choose Your Microrobot

When it comes to designing microrobots, the core element is their intended application. When developing future generations of light-powered microrobots, the first step should be to assess the key features needed for a specific task, and to select the type

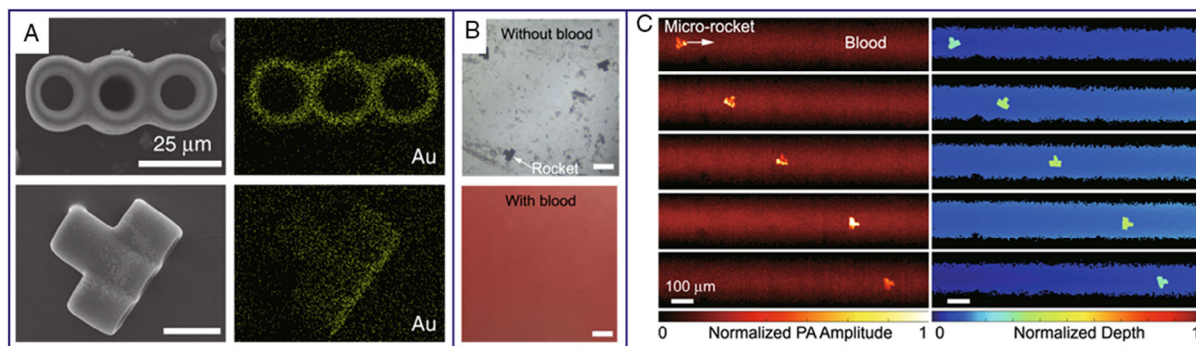
of microrobot accordingly. For example, in applications where extreme precision is essential, hard microrobots manipulated by optical trapping are likely to be the best choice, as optical trapping enables motion control with six degrees of freedom and nanometer precision. On the other hand, for applications where autonomy is important, microrobots made of smart materials are much more promising, because these can be engineered to allow for microrobotic motion or complex operations in response to local stimuli in liquids, as well as in dry environments. In addition, light can be used as actuator for triggering additional interesting effects, such as thermoplasmonic or photocatalytic effects, and light-triggered effects can be exploited for generating positive or negative phototaxis. Table 1 shows the aforementioned strategies for using light as a microrobot actuator.

The characteristics for the two main categories of light-controlled microrobots covered in this Review, i.e., hard polymeric microrobots and soft light-responsive polymeric microrobots, are compared in Table 2.

### 5.2. Ready, Set, Go—Where to?

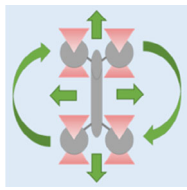
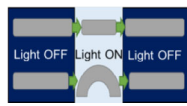
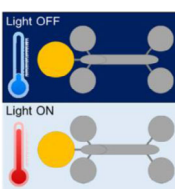
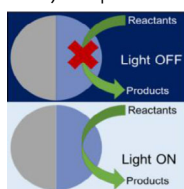
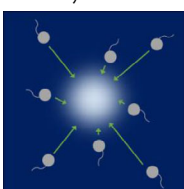
The ultimate goal in microrobotic research should be to mass-produce microrobots that can carry out their tasks autonomously, or that can be controlled by users with minimal training. In the particular case of light-powered microrobots, microrobots powered by common light sources (e.g., the sun or a household lamp) that can carry out a given task autonomously in a real-world environment (e.g., an environmental or biomedical sample) are highly desirable. Although such microrobots are still somewhere at the border with science fiction, research results in the field are currently laying the foundation for this work.

The cooperative and interactive action of multiple microrobots represents a fascinating challenge. At the microscale, this behavior has been principally studied for nanoparticles that in response to an external stimulus/gradient can cluster showing “schooling” behavior, or disperse exhibiting “exclusion” behavior.<sup>[48]</sup> Recently, hierarchical microswarms with leader-follower-like structures were also demonstrated: the self-organization and subsequent behavior of two different microparticle populations was induced by controlling local electrohydrodynamic and



**Figure 9.** Microrobot rockets and their photoacoustic imaging in a microchannel filled with bovine blood. A) Scanning electron micrographs (left) and energy dispersive X-ray spectrum (right) showing the microrobots from different angles. B) Optical microscopy of the microrockets with and without bovine blood. C) High-resolution photoacoustic tracking of a single-microrobot rocket in a microchannel with a 250 μm diameter filled with bovine blood: intensity distribution (left) and depth distribution (right). Reproduced under the terms of the CC-BY license.<sup>[178]</sup> Copyright 2020, The Authors, published by Springer Nature.

**Table 1.** Light as microrobot actuator: core strategies for microrobotic motion control and further activation mechanisms enabled by light.

Light as microrobot actuator				
Core strategies for controlling the motion of polymeric microrobots		Further activation mechanisms enabled by light		
<p><i>Optical trapping and manipulation</i> of rigid microrobots, which often include spherical handles, can be done with six degrees of freedom.</p> 	<p><i>Light-triggered shape changes</i> in soft stimuli-responsive microrobots can lead to various interesting microrobot motions and other operations when properly engineered.</p> 	<p><i>Thermoplasmonic effects</i>—heat is generated by illuminating a gold-coated microrobot component due to plasmon resonances.</p> 	<p><i>Photocatalytic effects</i>—chemical reactions occur only upon illumination, phenomenon often exploited on Janus particles.</p> 	<p><i>Phototaxis behaviors</i> inspired from nature can be exploited for microrobot motion toward the light source, or away from it.</p> 

**Table 2.** Comparison between different characteristics for polymeric light-powered hard and soft microrobots.

	Hard microrobots	Soft microrobots
Fabrication technique	DLW	DLW or photolithography
Fabrication scalability	Poor—serial fabrication process	Poor for DLW, good for photolithography
Materials	Acrylic- or epoxy-based negative photoresists, hybrid organic-inorganic materials	LCE, LCN, hydrogels, often in layered structures
Biocompatibility	Achievable, requires the use of biocompatible materials for fabrication	
Actuation mechanism	Direct—optical trapping	Indirect—based on light-induced shape changes
Robot dimensions	Several microns to tens of microns—limited by fabrication resolution	Tens or hundreds of microns—limited by resolution and material response to light
Actuation response time	Millisecond response timescale—limited by the optical trapping setup (hologram recalculation + SLM response time)	Millisecond operation timescale for LCE microrobots—limited by the material response
Precision of actuation	High, 6 degrees of freedom for the manipulation of microrobots with at least 3 trapping handles	Limited by the microrobot design and material properties
Power density at sample plane	Tens of mW per mm <sup>2</sup>	
Wavelength regime for the actuation source	nIR (typically around 1060–1090 nm)	UV and visible light (typically 200–700 nm)
Area where they can move	Limited by the field of view of the optical trapping setup to less than 1 × 1 mm <sup>2</sup> . Larger areas can be covered by displacing the sample.	No size restriction when flat light illumination can power the microrobot operation.
Manipulation scalability	Poor—limited by the field of view and number of optical traps that can be generated	High—microrobot operation can be induced by flat light illumination
Operating environment	Liquids, with challenges in complex media	Air and liquids, with challenges in complex media

diffusiophoretic interactions.<sup>[187]</sup> Although the nanoparticles investigated so far in these studies do not possess specific functions, fundamental studies on interacting microrobots would open to potential applications where they will accomplish the same or different tasks independently or triggered by mutual interactions and communication. While at the macroscale robot communication can take advantage of sensors, processors, and cabled or wireless routing, such components are difficult to integrate at the microscale within the tiny body of the microrobots. Microrobot communication could be instead based on physical or chemical fundamental interactions. A possible solution is to exploit magnetic forces that, on one hand, drive a dynamic self-assembly

of magnetic particles, and, on the other hand, rule the interactions among microrobots, mainly relying on magnetic repulsion of microrobots.<sup>[188]</sup> In this case, the interaction is constant without containing any feedback information of the operation of a single robot. This could be transferred to light-powered microrobots if an optical signal, such as lasing operation or diffraction of light, could be autonomously sent in between the microrobots in response to a user-programmed light activation, or to an environmental trigger signal such as a physical obstacle.

Alternatively, clever engineering solutions enabling extreme miniaturization of electronic components can be adopted, provided that these can be integrated into the microrobot



manufacturing process. Energy harvesting at the micro- and nanoscale is important for a number of applications, and microrobots could take advantage of developments in this field.<sup>[189]</sup> Therefore, an interesting technology that might prove crucial for the future of microrobots is that of nanogenerators, miniaturized devices that convert mechanical energy into electric power or signal. The different material strategies and system designs for wireless energy harvesting were recently reviewed in previous studies.<sup>[190]</sup> Piezoelectric,<sup>[191,192]</sup> triboelectric,<sup>[193–196]</sup> and pyroelectric<sup>[197,198]</sup> effects are most often exploited to scavenge energy in nanogenerator technologies. Hybridized nanogenerators exploiting intelligent combinations of the aforementioned effects, as well other effects, are also emerging.<sup>[199–201]</sup> In addition to energy harvesting, nanogenerators can also act as sensors enabling further applications.<sup>[202–204]</sup> Self-powered floating robotic insects with a size of a few centimeters were recently shown to move on the surface of water.<sup>[205]</sup> However, the concepts used for powering their motion are not directly transferrable to the microscale. On the other hand, silicon-based walking microrobots powered by a new class of actuators called surface electrochemical actuators were also recently demonstrated.<sup>[206]</sup> In principle, a similar type of on-board power could be achieved for light-controlled microrobots using conductive polymers for building the surface electrochemical actuator.

### 5.3. Envisioned Applications

This section discusses a number of potential future applications for light-powered microrobots, and the key characteristics that microrobots should have to accomplish the tasks involved. Biocompatibility is an underlying stringent requirement for all the envisioned applications mentioned herein, and the need for biocompatible materials is becoming more and more evident nowadays.<sup>[180,207]</sup> While some noncytotoxic photoresists for 2PP are already available, such as IP-Visio and Ormosil, more commercial and in-house biocompatible formulations are being developed.

Environmental applications should be extremely interesting for swarms of sun-powered microrobots. For example, water testing could be carried out using microrobots that cause a color change when encountering target toxic compounds or pathogens. Wastewater treatment in large water bodies, i.e., lakes or rivers, can also be envisioned with the aid of sun-powered “seek-and-destroy” microrobot swarms that catalyze decomposition of unwanted chemicals. The proof-of-concept experiments for such applications have already been successful,<sup>[21,51]</sup> but further developments are still needed before the concept can be applied on a large scale. Here, the mass-production and sun-powered aspects are critical. In addition, such microrobots need to be autonomous. Both requirements can be more easily achieved for relatively simple microrobots that are fueled by chemical reactions catalyzed by light.

A number of biomedical applications would benefit from the development of suitable microrobots. However, biological samples are complex and pose a number of challenges for using light as microrobot actuator.<sup>[58]</sup> Nevertheless, microrobots could prove useful for minimally invasive surgery in peripheral tissues, where focused light can penetrate, such as skin or cornea. In vitro

gene therapy with microrobot-enabled transfection is another interesting potential application. In this case, the microrobots would be user-controlled, the microrobot shapes would need to be rather complex, and the number of microrobots required would not be as high as for environmental applications. However, development and testing of microrobots for the specific applications described herein are needed. A nice proof-of-concept example is the microrobot reported by Kim et al. for eye surgery.<sup>[158]</sup> At this stage, we do not foresee the use of light-powered microrobots deep inside the human body due to the very limited tissue penetration of light. However, microrobots with hybrid magnetic and optical actuation could be suitable for performing tasks inside the human body.

In agriculture, microrobots could help improve gene transfection for the generation of genetically engineered plants with improved crop yields, resistance to pathogens, etc. For this purpose, the requirements are similar to those listed for biomedical applications.

## 6. Conclusion

The main purpose of this Review is to discuss the past, present, and future of light-powered microrobots. In the introduction, the study starts with a brief overview of the current applications of microrobots of various types in liquid environments. Different microrobot propulsion means and control modalities are then described. Particular emphasis is placed on fabrication and actuation using light. The review also discusses the current challenges in the field and potential solutions that, when successfully implemented, could turn light-powered microrobots into truly disruptive tools at the microscale. Finally, key elements in selecting and designing microrobots for new applications, and what these applications could be in the near future, are described.

With the increasing interest in microrobotics that has become obvious in recent years, it is expected that cooperation between different research fields related to microrobotics will flourish in the near future and lead to improved ideas and solutions to current challenges. This Review aims to serve as a starting point for connecting researchers working on different types of light-controlled polymeric microrobots. Integrating concepts from the parallel tracks on *hard* and *soft* polymeric microrobots is far from trivial, but it might prove to be a valuable solution for advancing light-controlled microrobots toward real-world applications. Combining different microrobotic components for a simultaneous or sequential light-based actuation might hold the key to enabling more complex applications for light-controlled microrobots, as well as increasing adaptability to real-world environments. In addition, using light in combination with an additional actuator could help overcome light-related challenges, as well as enable additional functionalities.

As current challenges encompass fabrication, actuation, biocompatibility and imaging issues, developments in the field of light-powered microrobots should benefit tremendously from interdisciplinary collaboration between experts in several scientific disciplines, including materials science, micro- and nanofabrication, optics and photonics, and data science. Ultimately, we believe that microrobots will successfully transition in the near future from interesting laboratory tools

to a technology with societal value, and that light will be one of the actuators powering the next generation of microrobots.

## Acknowledgements

A.-I.B. acknowledges financial support from VILLUM FONDEN (grant numbers 34424 and 00022918). Financial support from Ente Cassa di Risparmio di Firenze (2017/0713) is also acknowledged.

## Conflict of Interest

The authors declare no conflict of interest.

## Keywords

3D printing, microrobots, microswimmers, smart materials, two-photon polymerization

Received: November 11, 2020

Revised: December 17, 2020

Published online: February 22, 2021

- [1] E. W. H. Jager, O. Inganäs, I. Lundström, *Science* **2000**, *288*, 2335.
- [2] P. Galajda, P. Ormos, *Appl. Phys. Lett.* **2001**, *78*, 249.
- [3] M. E. J. Friese, H. Rubinsztein-Dunlop, J. Gold, P. Hagberg, D. Hanstorp, *Appl. Phys. Lett.* **2001**, *78*, 547.
- [4] W. F. Paxton, K. C. Kistler, C. C. Olmeda, A. Sen, S. K. St. Angelo, Y. Cao, T. E. Mallouk, P. E. Lammert, V. H. Crespi, *J. Am. Chem. Soc.* **2004**, *126*, 13424.
- [5] S. Fournier-Bidoz, A. C. Arsenault, I. Manners, G. A. Ozin, *Chem. Commun.* **2005**, 441.
- [6] R. Dreyfus, J. Baudry, M. L. Roper, M. Fermigier, H. A. Stone, J. Bibette, *Nature* **2005**, *437*, 862.
- [7] G. A. Ozin, I. Manners, S. Fournier-Bidoz, A. Arsenault, *Adv. Mater.* **2005**, *17*, 3011.
- [8] W. Gao, X. Feng, A. Pei, Y. Gu, J. Li, J. Wang, *Nanoscale* **2013**, *5*, 4696.
- [9] L. Soler, V. Magdanz, V. M. Fomin, S. Sanchez, O. G. Schmidt, *ACS Nano* **2013**, *7*, 9611.
- [10] F. Mou, C. Chen, H. Ma, Y. Yin, Q. Wu, J. Guan, *Angew. Chem., Int. Ed.* **2013**, *52*, 7208.
- [11] E. B. Steager, M. Selman Sakar, C. Magee, M. Kennedy, A. Cowley, V. Kumar, *Int. J. Rob. Res.* **2013**, *32*, 346.
- [12] A. I. Bunea, I. A. Pavel, S. David, S. Gáspár, *Biosens. Bioelectron.* **2015**, *67*, 42.
- [13] J. R. Baylis, J. H. Yeon, M. H. Thomson, A. Kazerooni, X. Wang, A. E. S. John, E. B. Lim, D. Chien, A. Lee, J. Q. Zhang, J. M. Piret, L. S. Machan, T. F. Burke, N. J. White, C. J. Kastrup, *Sci. Adv.* **2015**, *1*, e1500379.
- [14] J. Li, O. E. Shklyae, T. Li, W. Liu, H. Shum, I. Rozen, A. C. Balazs, J. Wang, *Nano Lett.* **2015**, *15*, 7077.
- [15] K. Villa, L. Krejčová, F. Novotný, Z. Heger, Z. Sofer, M. Pumera, *Adv. Funct. Mater.* **2018**, *28*, 1804343.
- [16] J. Li, P. Angsantikul, W. Liu, B. Esteban-Fernández de Ávila, X. Chang, E. Sandraz, Y. Liang, S. Zhu, Y. Zhang, C. Chen, W. Gao, L. Zhang, J. Wang, *Adv. Mater.* **2018**, *30*, 1.
- [17] J. Li, X. Li, T. Luo, R. Wang, C. Liu, S. Chen, D. Li, J. Yue, S. H. Cheng, D. Sun, *Sci. Robot.* **2018**, *3*, 1.
- [18] J. Park, C. Jin, S. Lee, J. Kim, H. Choi, *Adv. Healthcare Mater.* **2019**, *8*, 1900213.
- [19] I. Shishkin, H. Markovich, Y. Roichman, P. Ginzburg, *Micromachines* **2020**, *11*, 90.
- [20] F. Soto, J. Wang, R. Ahmed, U. Demirci, *Adv. Sci.* **2020**, *7*, 2002203.
- [21] L. Wang, A. Kaeppler, D. Fischer, J. Simmchen, *ACS Appl. Mater. Interfaces* **2019**, *11*, 32937.
- [22] B. J. Nelson, I. K. Kaliakatsos, J. J. Abbott, *Annu. Rev. Biomed. Eng.* **2010**, *12*, 55.
- [23] J. Li, B. E. F. De Ávila, W. Gao, L. Zhang, J. Wang, *Sci. Robot.* **2017**, *2*, eaam6431.
- [24] M. Luo, Y. Feng, T. Wang, J. Guan, *Adv. Funct. Mater.* **2018**, *28*, 1.
- [25] K. Kim, J. Guo, Z. Liang, D. Fan, *Adv. Funct. Mater.* **2018**, *28*, 1.
- [26] S. K. Srivastava, G. Clergeaud, T. L. Andresen, A. Boisen, *Adv. Drug* **2019**, *138*, 41.
- [27] J. Ye, D. A. Wilson, Y. Tu, F. Peng, *Adv. Mater. Technol.* **2020**, *5*, 2000435.
- [28] A.-I. Bunea, R. Taboryski, *Micromachines* **2020**, *11*, 1048.
- [29] W. Duan, W. Wang, S. Das, V. Yadav, T. E. Mallouk, A. Sen, *Annu. Rev. Anal. Chem.* **2015**, *8*, 311.
- [30] F. Wong, K. K. Dey, A. Sen, *Annu. Rev. Mater. Res.* **2016**, *46*, 407.
- [31] J. G. S. Moo, C. C. Mayorga-Martinez, H. Wang, B. Khezri, W. Z. Teo, M. Pumera, *Adv. Funct. Mater.* **2017**, *27*, 1604759.
- [32] H. Ceylan, J. Giltinan, K. Kozielski, M. Sitti, *Lab Chip* **2017**, *17*, 1705.
- [33] M. Safdar, S. U. Khan, J. Jänis, *Adv. Mater.* **2018**, *30*, 1703660.
- [34] Y. Zhang, K. Yuan, L. Zhang, *Adv. Mater. Technol.* **2019**, *4*, 1800636.
- [35] F. Mayer, S. Richter, J. Westhauser, E. Blasco, C. Barner-Kowollik, M. Wegener, *Sci. Adv.* **2019**, *5*, eaau9160.
- [36] A. C. H. Tsang, E. Demir, Y. Ding, O. S. Pak, *Adv. Intell. Syst.* **2020**, *2*, 1900137.
- [37] Y. Tu, F. Peng, D. A. Wilson, *Adv. Mater.* **2017**, *29*, 1701970.
- [38] H. Wang, M. Pumera, *Adv. Funct. Mater.* **2018**, *28*, 1.
- [39] Y. Alapan, O. Yasa, B. Yigit, I. C. Yasa, P. Erkok, M. Sitti, *Annu. Rev. Control. Robot. Auton. Syst.* **2019**, *2*, 205.
- [40] R. S. M. Rikken, R. J. M. Nolte, J. C. Maan, J. C. M. Van Hest, D. A. Wilson, P. C. M. Christianen, *Soft Matter* **2014**, *10*, 1295.
- [41] M. Sitti, D. S. Wiersma, *Adv. Mater.* **2020**, *32*, 1906766.
- [42] X. Z. Chen, M. Hoop, F. Mushtaq, E. Siringil, C. Hu, B. J. Nelson, S. Pané, *Appl. Mater. Today* **2017**, *9*, 37.
- [43] S. Fusco, H. W. Huang, K. E. Peyer, C. Peters, M. Häberli, A. Ulbers, A. Spyrogiani, E. Pellicer, J. Sort, S. E. Pratsinis, B. J. Nelson, M. S. Sakar, S. Pané, *ACS Appl. Mater. Interfaces* **2015**, *7*, 6803.
- [44] J. Li, T. Li, T. Xu, M. Kiristi, W. Liu, Z. Wu, J. Wang, *Nano Lett.* **2015**, *15*, 4814.
- [45] H. Li, G. Go, S. Y. Ko, J. O. Park, S. Park, *Smart Mater. Struct.* **2016**, *25*, 027001.
- [46] G. Go, V. Du Nguyen, Z. Jin, J. O. Park, S. Park, *Int. J. Control. Autom. Syst.* **2018**, *16*, 1341.
- [47] S. Sengupta, M. E. Ibele, A. Sen, *Angew. Chem., Int. Ed.* **2012**, *51*, 8434.
- [48] W. Wang, W. Duan, S. Ahmed, T. E. Mallouk, A. Sen, *Nano Today* **2013**, *8*, 531.
- [49] I.-A. Pavel, A.-I. Bunea, S. David, S. Gáspár, *ChemCatChem* **2014**, *6*, 866.
- [50] S. Gáspár, *Nanoscale* **2014**, *6*, 7757.
- [51] J. Li, V. V. Singh, S. Sattayasamitsathit, J. Orozco, K. Kaufmann, R. Dong, W. Gao, B. Jurado-Sanchez, Y. Fedorak, J. Wang, *ACS Nano* **2014**, *8*, 11118.
- [52] B. Esteban-Fernández de Ávila, P. Angsantikul, J. Li, W. Gao, L. Zhang, J. Wang, *Adv. Funct. Mater.* **2018**, *28*, 1.
- [53] K. Han, C. W. Shields, O. D. Velev, *Adv. Funct. Mater.* **2018**, *28*, 1.
- [54] M. Kaynak, P. Dirix, M. S. Sakar, *Adv. Sci.* **2020**, *7*, 2001120.
- [55] E. Gultepe, J. S. Randhawa, S. Kadam, S. Yamanaka, F. M. Selaru, E. J. Shin, A. N. Kalloo, D. H. Gracias, *Adv. Mater.* **2013**, *25*, 514.

- [56] J. C. Breger, C. Yoon, R. Xiao, H. R. Kwag, M. O. Wang, J. P. Fisher, T. D. Nguyen, D. H. Gracias, *ACS Appl. Mater. Interfaces* **2015**, 7, 3398.
- [57] A. Ashkin, *Phys. Rev. Lett.* **1970**, 24, 156.
- [58] A.-I. Bunea, J. Glückstad, *Laser Photonics Rev.* **2019**, 13, 1800227.
- [59] D. Martella, S. Nocentini, F. Micheletti, D. S. Wiersma, C. Parmeggiani, *Soft Matter* **2019**, 15, 1312.
- [60] P. Weis, S. Wu, *Macromol. Rapid Commun.* **2018**, 39, 1700220.
- [61] M. Hippler, E. Blasco, J. Qu, M. Tanaka, C. Barner-Kowollik, M. Wegener, M. Bastmeyer, *Nat. Commun.* **2019**, 10, 1.
- [62] H. Zeng, P. Wasylczyk, C. Parmeggiani, D. Martella, M. Burrese, D. S. Wiersma, *Adv. Mater.* **2015**, 27, 3883.
- [63] E. Engay, A.-I. Bunea, M. Chouliara, A. Bañas, J. Glückstad, *Opt. Lett.* **2018**, 43, 3870.
- [64] J. Zheng, B. Dai, J. Wang, Z. Xiong, Y. Yang, J. Liu, X. Zhan, Z. Wan, J. Tang, *Nat. Commun.* **2017**, 8, 1438.
- [65] M. Reicherter, T. Haist, E. U. Wagemann, H. J. Tiziani, *Opt. Lett.* **1999**, 24, 608.
- [66] J. Liesener, M. Reicherter, T. Haist, H. J. Tiziani, *Opt. Commun.* **2000**, 185, 77.
- [67] J. E. Curtis, B. A. Koss, D. G. Grier, *Opt. Commun.* **2002**, 207, 169.
- [68] H.-U. Ulriksen, J. Thogersen, S. Keiding, I. R. Perch-Nielsen, J. S. Dam, D. Z. Palima, H. Stapelfeldt, J. Glückstad, *J. Eur. Opt. Soc. Rapid Publ.* **2008**, 3, 08034.
- [69] S. Tauro, A. Bañas, D. Palima, J. Glückstad, *Opt. Express* **2011**, 19, 7106.
- [70] E. Avcı, M. Grammatikopoulou, G.-Z. Yang, *Adv. Opt. Mater.* **2017**, 5, 1700031.
- [71] D. Zhang, A. Barbot, B. Lo, G. Yang, *Adv. Opt. Mater.* **2020**, 8, 2000543.
- [72] P. Y. Chiou, A. T. Ohta, M. C. Wu, *Nature* **2005**, 436, 370.
- [73] S. Zhang, Y. Liu, Y. Qian, W. Li, J. Juvert, P. Tian, J.-C. Navarro, A. W. Clark, E. Gu, M. D. Dawson, J. M. Cooper, S. L. Neale, *Opt. Express* **2017**, 25, 28838.
- [74] S. Zhang, N. Shakiba, Y. Chen, Y. Zhang, P. Tian, J. Singh, M. D. Chamberlain, M. Satkauskas, A. G. Flood, N. P. Kherani, S. Yu, P. W. Zandstra, A. R. Wheeler, *Small* **2018**, 14, 1803342.
- [75] S. Zhang, E. Y. Scott, J. Singh, Y. Chen, Y. Zhang, M. Elsayed, M. Dean Chamberlain, N. Shakiba, K. Adams, S. Yu, C. M. Morshead, P. W. Zandstra, A. R. Wheeler, *Proc. Natl. Acad. Sci.* **2019**, 116, 14823.
- [76] M. Göppert-Mayer, *Ann. Phys.* **1931**, 401, 273.
- [77] W. Kaiser, C. G. B. Garrett, *Phys. Rev. Lett.* **1961**, 7, 229.
- [78] S. Maruo, O. Nakamura, S. Kawata, *Opt. Lett.* **2017**, 22, 132.
- [79] Y. L. Zhang, Q. D. Chen, H. Xia, H. B. Sun, *Nano Today* **2010**, 5, 435.
- [80] J. Fischer, M. Wegener, *Laser Photonics Rev.* **2013**, 7, 22.
- [81] Y. Bougdid, Z. Sekkat, *Sci. Rep.* **2020**, 10, 10409.
- [82] R. A. Farrer, C. N. LaFratta, L. Li, J. Praino, M. J. Naughton, B. E. A. Saleh, M. C. Teich, J. T. Fourkas, *J. Am. Chem. Soc.* **2006**, 128, 1796.
- [83] G. Vizsnyczai, J. Joniova, B. L. Aekbote, A. Strejc, P. Ormos, P. Miskovsky, L. Kelemen, G. Báno, *Langmuir* **2015**, 11, 23.
- [84] H. Ceylan, I. C. Yasa, M. Sitti, *Adv. Mater.* **2017**, 29, 1605072.
- [85] B. L. Aekbote, J. Jacak, G. J. Schütz, E. Csányi, Z. Szegletes, P. Ormos, L. Kelemen, *Eur. Polym. J.* **2012**, 48, 1745.
- [86] A. I. Bunea, M. H. Jakobsen, E. Engay, A. R. Bañas, J. Glückstad, *Micro Nano Eng.* **2019**, 2, 41.
- [87] M. J. Villangca, D. Palima, A. R. Bañas, J. Glückstad, *Light Sci. Appl.* **2016**, 5, e16148.
- [88] C. A. Spiegel, M. Hippler, A. Münchinger, M. Bastmeyer, C. Barner-Kowollik, M. Wegener, E. Blasco, *Adv. Funct. Mater.* **2020**, 30, 1907615.
- [89] A. Nishiguchi, H. Zhang, S. Schweizerhof, M. F. Schulte, A. Mourran, M. Möller, *ACS Appl. Mater. Interfaces* **2020**, 12, 12176.
- [90] J. del Barrio, C. Sánchez-Somolinos, *Adv. Opt. Mater.* **2019**, 7, 1900598.
- [91] M. Del Pozo, C. Delaney, C. W. M. Bastiaansen, D. Diamond, A. P. H. J. Schenning, L. Florea, *ACS Nano* **2020**, 14, 9832.
- [92] C. Barner-Kowollik, M. Bastmeyer, E. Blasco, G. Delaittre, P. Müller, B. Richter, M. Wegener, *Angew. Chem., Int. Ed.* **2017**, 56, 15828.
- [93] F. Mayer, D. Ryklin, I. Wacker, R. Curticean, M. Čalkovský, A. Niemeyer, Z. Dong, P. A. Levkin, D. Gerthsen, R. R. Schröder, M. Wegener, *Adv. Mater.* **2020**, 32, 2002044.
- [94] D. Gräfe, A. Wickberg, M. M. Zieger, M. Wegener, E. Blasco, C. Barner-Kowollik, *Nat. Commun.* **2018**, 9, 1.
- [95] M. M. Zieger, P. Müller, E. Blasco, C. Petit, V. Hahn, L. Michalek, H. Mutlu, M. Wegener, C. Barner-Kowollik, *Adv. Funct. Mater.* **2018**, 28, 1801405.
- [96] R. Batchelor, T. Messer, M. Hippler, M. Wegener, C. Barner-Kowollik, E. Blasco, *Adv. Mater.* **2019**, 31, 1904085.
- [97] X. Wang, X.-H. Qin, C. Hu, A. Terzopoulou, X.-Z. Chen, T.-Y. Huang, K. Maniura-Weber, S. Pané, B. J. Nelson, *Adv. Funct. Mater.* **2018**, 28, 1804107.
- [98] D. Gräfe, M. Gernhardt, J. Ren, E. Blasco, M. Wegener, M. A. Woodruff, C. Barner-Kowollik, *Adv. Funct. Mater.* **2021**, 31, 2006998.
- [99] J. S. Oakdale, J. Ye, W. L. Smith, J. Biener, *Opt. Express* **2016**, 24, 27077.
- [100] M. Gernhardt, E. Blasco, M. Hippler, J. Blinco, M. Bastmeyer, M. Wegener, H. Frisch, C. Barner-Kowollik, *Adv. Mater.* **2019**, 31, 1901269.
- [101] N. Chidambaram, R. Kirchner, R. Fallica, L. Yu, M. Altana, H. Schift, *Adv. Mater. Technol.* **2017**, 2, 1700018.
- [102] G. Seniutinas, A. Weber, C. Padeste, I. Sakellari, M. Farsari, C. David, *Microelectron. Eng.* **2018**, 191, 25.
- [103] S. Maruo, A. Takaura, Y. Saito, *Opt. Express* **2009**, 17, 18525.
- [104] T. Asavei, V. L. Y. Loke, M. Barbieri, T. A. Nieminen, N. R. Heckenberg, H. Rubinsztein-Dunlop, *New J. Phys.* **2009**, 11, 093021.
- [105] D. B. Phillips, M. J. Padgett, S. Hanna, Y.-L. D. Ho, D. M. Carberry, M. J. Miles, S. H. Simpson, *Nat. Photonics* **2014**, 8, 400.
- [106] J. Köhler, S. I. Ksouri, C. Esen, A. Ostendorf, *Microsyst. Nanoeng.* **2017**, 3, 16083.
- [107] J. Köhler, Y. Kutlu, G. Zyla, S. I. Ksouri, C. Esen, E. L. Gurevich, A. Ostendorf, *Opt. Eng.* **2017**, 56, 1.
- [108] L. J. Jiang, Y. S. Zhou, W. Xiong, Y. Gao, X. Huang, L. Jiang, T. Baldacchini, J.-F. Silvain, Y. F. Lu, *Opt. Lett.* **2014**, 39, 3034.
- [109] D. B. Phillips, G. M. Gibson, R. Bowman, M. J. Padgett, S. Hanna, D. M. Carberry, M. J. Miles, S. H. Simpson, *Opt. Express* **2012**, 20, 29679.
- [110] B. L. Aekbote, T. Fekete, J. Jacak, G. Vizsnyczai, P. Ormos, L. Kelemen, *Biomed. Opt. Express* **2016**, 7, 45.
- [111] U. G. Bütaitė, G. M. Gibson, Y. L. D. Ho, M. Taverne, J. M. Taylor, D. B. Phillips, *Nat. Commun.* **2019**, 10, 1215.
- [112] S. Hu, R. Hu, X. Dong, T. Wei, S. Chen, D. Sun, *Opt. Express* **2019**, 27, 16475.
- [113] I. Grexa, T. Fekete, J. Molnár, K. Molnár, G. Vizsnyczai, P. Ormos, L. Kelemen, *Micromachines* **2020**, 11, 882.
- [114] D. Palima, A. R. Bañas, G. Vizsnyczai, L. Kelemen, P. Ormos, J. Glückstad, *Opt. Express* **2012**, 20, 2004.
- [115] W. Lamperska, S. Drobczyński, M. Nawrot, P. Wasylczyk, J. Masajada, W. Lamperska, S. Drobczyński, M. Nawrot, P. Wasylczyk, J. Masajada, *Micromachines* **2018**, 9, 277.
- [116] M. Medina-Sánchez, V. Magdanz, M. Guix, V. M. Fomin, O. G. Schmidt, *Adv. Funct. Mater.* **2018**, 28, 1707228.
- [117] S. Palagi, D. P. Singh, P. Fischer, *Adv. Opt. Mater.* **2019**, 7, 1900370.

- [118] N. El-Atab, R. B. Mishra, F. Al-Modaf, L. Joharji, A. A. Alsharif, H. Alamoudi, M. Diaz, N. Qaiser, M. M. Hussain, *Adv. Intell. Syst.* **2020**, *2*, 2000128.
- [119] M. Hippler, E. Blasco, J. Qu, M. Tanaka, C. Barner-Kowollik, M. Wegener, M. Bastmeyer, *Nat. Commun.* **2019**, *10*, 1.
- [120] R. A. M. Hikmet, D. J. Broer, *Polymer* **1991**, *32*, 1627.
- [121] D. Shah, B. Yang, S. Kriegman, M. Levin, J. Bongard, R. Kramer-Bottiglio, *Adv. Mater.* **2020**, 2002882.
- [122] S. Nocentini, C. Parmeggiani, D. Martella, D. S. Wiersma, *Adv. Opt. Mater.* **2018**, *6*, 1800207.
- [123] Y. Hirokawa, T. Tanaka, *J. Chem. Phys.* **1984**, *81*, 6379.
- [124] S. Fusco, M. S. Sakar, S. Kennedy, C. Peters, R. Bottani, F. Starsich, A. Mao, G. A. Sotiriou, S. Pané, S. E. Pratsinis, D. Mooney, B. J. Nelson, *Adv. Mater.* **2014**, *26*, 952.
- [125] E. M. Purcell, *Am. J. Phys.* **1977**, *45*, 3.
- [126] H. Zhang, A. Mourran, M. Möller, *Nano Lett.* **2017**, *17*, 2010.
- [127] A. Mourran, H. Zhang, R. Vinokur, M. Möller, *Adv. Mater.* **2017**, *29*, 1604825.
- [128] H. Zhang, L. Koens, E. Lauga, A. Mourran, M. Möller, *Small* **2019**, *15*, 1903379.
- [129] I. Rehor, C. Maslen, P. G. Moerman, B. G. P. van Ravensteyn, R. van Alst, J. Groenewold, H. B. Eral, W. K. Kegel, *Soft Robot.* **2020**, <https://doi.org/10.1089/soro.2019.0169>.
- [130] C. J. Barrett, J. I. Mamiya, K. G. Yager, T. Ikeda, *Soft Matter* **2007**, *3*, 1249.
- [131] C. Ohm, M. Brehmer, R. Zentel, *Adv. Mater.* **2010**, *22*, 3366.
- [132] H. Yu, T. Ikeda, *Adv. Mater.* **2011**, *23*, 2149.
- [133] T. J. White, D. J. Broer, *Nat. Mater.* **2015**, *14*, 1087.
- [134] S. Palagi, A. G. Mark, S. Y. Reigh, K. Melde, T. Qiu, H. Zeng, C. Parmeggiani, D. Martella, A. Sanchez-castillo, N. Kapernaum, F. Giesselmann, D. S. Wiersma, E. Lauga, P. Fischer, *Nat. Mater.* **2016**, *15*, 647.
- [135] B. A. Kowalski, T. C. Guin, A. D. Auguste, N. P. Godman, T. J. White, *ACS Macro Lett.* **2017**, *6*, 436.
- [136] L. T. De Haan, A. P. H. J. Schenning, D. J. Broer, *Polymer* **2014**, *55*, 5885.
- [137] Y. Shang, J. Wang, T. Ikeda, L. Jiang, *J. Mater. Chem. C* **2019**, *7*, 3413.
- [138] M. Pilz da Cunha, M. G. Debije, A. P. H. J. Schenning, *Chem. Soc. Rev.* **2020**, *49*, 6568.
- [139] S. Nocentini, D. Martella, D. S. Wiersma, C. Parmeggiani, *Soft Matter* **2017**, *13*, 8590.
- [140] H. Zeng, D. Martella, P. Wasylczyk, G. Cerretti, J. C. G. Lavocat, C. H. Ho, C. Parmeggiani, D. S. Wiersma, *Adv. Mater.* **2014**, *26*, 2319.
- [141] S. Nocentini, D. Martella, C. Parmeggiani, D. S. Wiersma, *Materials* **2016**, *9*, 525.
- [142] H. Zeng, P. Wasylczyk, G. Cerretti, D. Martella, C. Parmeggiani, D. S. Wiersma, *Appl. Phys. Lett.* **2015**, *106*, 111902.
- [143] D. Martella, S. Nocentini, D. Nuzhdin, C. Parmeggiani, D. S. Wiersma, *Adv. Mater.* **2017**, *29*, 1704047.
- [144] D. Martella, D. Antonioli, S. Nocentini, D. S. Wiersma, G. Galli, M. Laus, C. Parmeggiani, *RSC Adv.* **2017**, *7*, 19940.
- [145] D. S. Wiersma, C. Parmeggiani, *Polymers* **2019**, *11*, 1644.
- [146] M. Lattuada, T. A. Hatton, *Nano Today* **2011**, *6*, 286.
- [147] G. A. Swartzlander, T. J. Peterson, A. B. Artusio-Glimpse, A. D. Raisanen, *Nat. Photonics* **2011**, *5*, 48.
- [148] A. B. Artusio-Glimpse, T. J. Peterson, G. A. Swartzlander, *Opt. Lett.* **2013**, *38*, 935.
- [149] T. Wu, T. A. Nieminen, S. Mohanty, J. Miotke, R. L. Meyer, H. Rubinsztein-Dunlop, M. W. Berns, *Nat. Photonics* **2012**, *6*, 62.
- [150] L. Shao, M. Käll, *Adv. Funct. Mater.* **2018**, *28*, 1.
- [151] C. Chen, F. Mou, L. Xu, S. Wang, J. Guan, Z. Feng, Q. Wang, L. Kong, W. Li, J. Wang, Q. Zhang, *Adv. Mater.* **2017**, *29*, 1603374.
- [152] Y. Ying, A. M. Pourrahimi, C. L. Manzaneres-Palenzuela, F. Novotny, Z. Sofer, M. Pumera, *Small* **2020**, *16*, 1902944.
- [153] K. Villa, L. Děkanovský, J. Plutnar, J. Kosina, M. Pumera, *Adv. Funct. Mater.* **2020**, *30*, 2007073.
- [154] S. Du, H. Wang, C. Zhou, W. Wang, Z. Zhang, *J. Am. Chem. Soc.* **2020**, *142*, 2213.
- [155] R. Dong, Y. Hu, Y. Wu, W. Gao, B. Ren, Q. Wang, Y. Cai, *J. Am. Chem. Soc.* **2017**, *139*, 1722.
- [156] V. Sridhar, B. W. Park, S. Guo, P. A. Van Aken, M. Sitti, *ACS Appl. Mater. Interfaces* **2020**, *12*, 24149.
- [157] H. Xin, N. Zhao, Y. Wang, X. Zhao, T. Pan, Y. Shi, B. Li, *Nano Lett.* **2020**.
- [158] M. Kim, H. Lee, S. Ahn, *Adv. Mater. Technol.* **2019**, *4*, 1900583.
- [159] Y. Y. Tanaka, P. Albella, M. Rahmani, V. Giannini, S. A. Maier, T. Shimura, *Sci. Adv.* **2020**, *6*, eabc3726.
- [160] L. Xu, F. Mou, H. Gong, M. Luo, J. Guan, *Chem. Soc. Rev.* **2017**, *46*, 6905.
- [161] Z. C. Ma, Y. L. Zhang, B. Han, X. Y. Hu, C. H. Li, Q. D. Chen, H. B. Sun, *Nat. Commun.* **2020**, *11*, 4536.
- [162] J. Giltinan, P. Katsamba, W. Wang, E. Lauga, M. Sitti, *Appl. Phys. Lett.* **2020**, *116*, 134101.
- [163] M. Lahikainen, H. Zeng, A. Priimagi, *Soft Matter* **2020**.
- [164] A. Najafi, R. Golestanian, *Phys. Rev. E* **2004**, *69*, 4.
- [165] A. C. H. Tsang, P. W. Tong, S. Nallan, O. S. Pak, *Phys. Rev. Fluids* **2020**, *5*, 074101.
- [166] K. Doya, *Neural Comput.* **2000**, *12*, 219.
- [167] J. Kober, J. A. Bagnell, J. Peters, *Int. J. Rob. Res.* **2013**, *32*, 1238.
- [168] I. M. Vellekoop, A. P. Mosk, *Opt. Commun.* **2008**, *281*, 3071.
- [169] T. Peng, R. Li, S. An, X. Yu, M. Zhou, C. Bai, Y. Liang, M. Lei, C. Zhang, B. Yao, P. Zhang, *Opt. Express* **2019**, *27*, 4858.
- [170] Y. Liu, C. Ma, Y. Shen, J. Shi, L. V. Wang, *Optica* **2017**, *4*, 280.
- [171] K. Zhang, Z. Wang, H. Zhao, C. Liu, H. Zhang, B. Xue, *Appl. Sci.* **2020**, *10*, 875.
- [172] A. Von Rohr, S. Trimpe, A. Marco, P. Fischer, S. Palagi, in *Int. Conf. on Intelligent Robots and Systems*, Institute of Electrical and Electronics Engineers Inc., Madrid, Spain **2018**, pp. 6199–6206.
- [173] S. Colabrese, K. Gustavsson, A. Celani, L. Biferale, *Phys. Rev. Lett.* **2017**, *118*, 158004.
- [174] Y. Zhao, X.-X. Liu, A. Alù, *J. Opt.* **2014**, *16*, 123001.
- [175] A. Li, S. Singh, D. Sievenpiper, *Nanophotonics* **2018**, *7*, 989.
- [176] A.-I. Bunea, M. Chouliara, S. Harloff-Helleberg, A. R. Bañas, E. L. Engay, J. Glückstad, *J. Biomed. Opt.* **2019**, *24*, 1.
- [177] P. Cabanach, A. Pena-Francesch, D. Sheehan, U. Bozuyuk, O. Yasa, S. Borros, M. Sitti, *Adv. Mater.* **2020**, *32*, 2003013.
- [178] D. Li, C. Liu, Y. Yang, L. Wang, Y. Shen, *Light Sci. Appl.* **2020**, *9*, 84.
- [179] M. Pilz Da Cunha, E. A. J. Van Thoor, M. G. Debije, D. J. Broer, A. P. H. J. Schenning, *J. Mater. Chem. C* **2019**, *7*, 13502.
- [180] J. Ou, K. Liu, J. Jiang, D. A. Wilson, L. Liu, F. Wang, S. Wang, Y. Tu, F. Peng, *Small* **2020**, *16*, 2070152.
- [181] D. Martella, P. Paoli, J. M. Pioner, L. Sacconi, R. Coppini, L. Santini, M. Lulli, E. Cerbai, D. S. Wiersma, C. Poggese, C. Ferrantini, C. Parmeggiani, *Small* **2017**, *13*, 1702677.
- [182] D. Martella, L. Pattelli, C. Matassini, F. Ridi, M. Bonini, P. Paoli, P. Baglioni, D. S. Wiersma, C. Parmeggiani, *Adv. Healthcare Mater.* **2019**, *8*, 1970009.
- [183] I. C. Yasa, H. Ceylan, U. Bozuyuk, A. M. Wild, M. Sitti, *Sci. Robot.* **2020**, *5*, 111334.
- [184] A. Halder, Y. Sun, *Biosens. Bioelectron.* **2019**, *139*, 111334.
- [185] S. Pané, J. Puigmartí-Luis, C. Bergeles, X. Chen, E. Pellicer, J. Sort, V. Počepcová, A. Ferreira, B. J. Nelson, *Adv. Mater. Technol.* **2019**, *4*, 1800575.
- [186] C. A. Koepele, M. Guix, C. Bi, G. Adam, D. J. Cappelleri, *Adv. Intell. Syst.* **2020**, *2*, 1900147.

- [187] X. Liang, F. Mou, Z. Huang, J. Zhang, M. You, L. Xu, M. Luo, J. Guan, *Adv. Funct. Mater.* **2020**, *30*, 1908602.
- [188] B. Yigit, Y. Alapan, M. Sitti, *Adv. Sci.* **2019**, *6*, 1801837.
- [189] Z. L. Wang, W. Wu, *Angew. Chem., Int. Ed.* **2012**, *51*, 11700.
- [190] L. Jiang, Y. Yang, Y. Chen, Q. Zhou, *Nano Energy* **2020**, *77*, 105131.
- [191] J. Briscoe, S. Dunn, *Nano Energy* **2014**, *14*, 15.
- [192] N. Sezer, M. Koç, *Nano Energy* **2021**, *80*, 105567.
- [193] F. R. Fan, Z. Q. Tian, Z. Lin Wang, *Nano Energy* **2012**, *1*, 328.
- [194] Z. L. Wang, *ACS Nano* **2013**, *7*, 9533.
- [195] Y. Su, Y. Yang, X. Zhong, H. Zhang, Z. Wu, Y. Jiang, Z. L. Wang, *ACS Appl. Mater. Interfaces* **2014**, *6*, 553.
- [196] H. Zhang, L. Yao, L. Quan, X. Zheng, *Nanotechnol. Rev.* **2020**, *9*, 610.
- [197] H. Ryu, S. Kim, *Small* **2019**, 1903469.
- [198] R. A. Surmenev, R. V. Chernozem, I. O. Pariy, M. A. Surmeneva, *Nano Energy* **2021**, *79*, 105442.
- [199] K. Zhang, S. Wang, Y. Yang, *Adv. Energy Mater.* **2017**, *7*, 1601852.
- [200] T. Zhang, T. Yang, M. Zhang, C. R. Bowen, Y. Yang, *iScience* **2020**, *23*, 101689.
- [201] L. S. G. Zhou, F. Qin, L. Li, W. Song, Z. Sun, *Nat. Commun.* **2020**, *11*, 6158.
- [202] D. Zhang, S. Xu, X. Zhao, W. Qian, C. R. Bowen, Y. Yang, *Adv. Funct. Mater.* **2020**, *30*, 1910809.
- [203] Y. Wang, H. Wu, L. Xu, H. Zhang, Y. Yang, Z. L. Wang, *Sci. Adv.* **2020**, *6*, eabb9083.
- [204] T. Jin, Z. Sun, L. Li, Q. Zhang, M. Zhu, Z. Zhang, G. Yuan, T. Chen, Y. Tian, X. Hou, C. Lee, *Nat. Commun.* **2020**, *11*, 5381.
- [205] Y. Wang, Y. Jiang, H. Wu, Y. Yang, *Nano Energy* **2019**, *63*, 103810.
- [206] M. Z. Miskin, A. J. Cortese, K. Dorsey, E. P. Esposito, M. F. Reynolds, Q. Liu, M. Cao, D. A. Muller, P. L. McEuen, I. Cohen, *Nature* **2020**, *584*, 557.
- [207] C. Delaney, N. Geoghegan, H. Ibrahim, M. O'Loughlin, B. J. Rodriguez, L. Florea, S. M. Kelleher, *ACS Appl. Polym. Mater.* **2020**, *2*, 3632.
- [208] A.-I. Bunea, E. Engay, M. Chouliara, A. R. Bañas, J. Glückstad, in *Advanced Manufacturing Technologies for Micro- and Nanosystems in Security and Defence* (Eds: A. Camposo, Y. Dzenis, M. Farsari, L. Persano), SPIE **2018**, p. 1080406.



**Ada-Ioana Bunea** got her Ph.D. degree in Micro- and Nanotechnology from the Technical University of Denmark, DTU Nanotech, in 2018. She is currently working as a postdoctoral researcher at DTU Nanolab and is principal investigator on two research projects focused on light-powered microrobots. Originally trained as a chemist at the University of Bucharest, in Romania, her background is highly interdisciplinary, combining expertise in fabrication, surface modification and various characterization techniques.



**Daniele Martella** got his Ph.D. (Doctor Europaeus) degree in Chemical Science in Firenze, Italy, in 2015, with Prof. A. Goti, after spending 7 months at the University of Zaragoza, Spain, with Prof. L. Oriol and Dr. M. Piñol. Since 2020, he is researcher at the National Institute for Metrological Research (INRiM), Italy. His research interest focuses on the synthesis and characterization of LCs and other smart materials for microrobotics, biological, and optical applications.



**Sara Nocentini** got her International Doctorate in Atomic and Molecular Photonics in Firenze, in 2017 with Prof. D. S. Wiersma. From 2017, she was a postdoctoral fellow at the European Laboratory for nonlinear spectroscopy, and in 2019, she joined the National Institute for Metrological Research as a researcher. Her research interests focus on polymeric optically reconfigurable materials as liquid crystal and LCNs for tunable photonics and microrobotics.



**Diederik S. Wiersma** received his Ph.D. degree in Amsterdam, The Netherlands, in 1995. Currently, he is physics professor at the University of Florence, Italy, head of the Micro and Nano Photonics research area at the European Laboratory for Non-Linear Spectroscopy (LENS), and president of the National Metrology Institute INRiM, Italy. His research interests lie in the fundamental optical properties of photonic materials and their practical applications.